

Phase Behavior and Reliable Computation of High Pressure Solid-Fluid Equilibrium with Cosolvents

Aaron M. Scurto[†], Gang Xu[‡], Joan F. Brennecke^{*} and Mark A. Stadtherr

Department of Chemical and Biomolecular Engineering
University of Notre Dame
182 Fitzpatrick Hall
Notre Dame, IN 46556
USA

[†]Current Address: Institut für Technische Chemie und Makromolekulare Chemie, RWTH-Aachen, Worringerweg 1, Aachen, D-52074, Germany

[‡]Current Address: SimSci-Esscor/Invensys, 26561 Rancho Parkway South, Suite 100, Lake Forest, CA 92630

^{*}Author to whom correspondence should be addressed: Tel.: (574) 631-5847, Fax: (574) 631-8366, E-mail: jfb@nd.edu

(February 2003)

(revised, June 2003)

Abstract

The identification of the correct, stable solution to a phase equilibrium problem, given a particular thermodynamic model, is essential for the design of separation processes. It is also important in the selection of an appropriate model to represent experimental data. The need for a completely reliable method to test for phase stability is particularly pressing when the number of phases likely to be present is not intuitive to the user, as is frequently the case with high-pressure systems. Previously, we have presented a completely reliable computational technique, based on interval analysis, to correctly identify phase equilibrium and test for phase stability in binary solvent-solute systems, that include the possibility of a solid phase, using any of a variety of cubic equations of state as the thermodynamic model. Here we extend the methodology to include multicomponent solvent-solute-cosolvent systems where the likelihood of additional phase formation is even greater than in the binary case. Gaseous or liquid cosolvents are frequently used in supercritical fluid extraction processes, and are integral in processes such as the gas anti-solvent process (GAS) to precipitate uniform solid particles. Using several examples from the literature, we demonstrate how the new computational technique can be used to identify experimental data that may have been misinterpreted and to identify models that do not predict what the modeler intended.

Keywords: Solid-Fluid Equilibrium, Supercritical Fluids, Phase Stability, Phase Equilibrium, Interval Analysis

1. INTRODUCTION

The calculation of solid-fluid equilibrium using an equation of state has formed the foundation for the design of supercritical fluid extraction processes.¹ It is also important in designing solid precipitation processes using high-pressure gases, such as the rapid expansion of a supercritical solution (RESS), gas anti-solvent (GAS) and supercritical anti-solvent (SAS) processes.^{2,3,4,5,6} In a previous paper⁷ we presented a framework for the completely reliable computation of solid-fluid equilibrium, using interval analysis to solve correctly the phase equilibrium and phase stability problems, when a cubic equation of state is used as the thermodynamic model for binary solvent-solute systems. We chose to apply the technique using cubic equations of state because they are simple, generally give good representations of high-pressure phase behavior, and are used extensively in industry. In this paper we extend this framework for the reliable computation of solid-fluid equilibrium to *multicomponent* solvent-solute-cosolvent mixtures.

The *correct* solution of multicomponent high-pressure phase equilibrium problems involving solids is vitally important to process design and to the evaluation of model performance. Without the identification of the correct, thermodynamically stable solutions to a model, experimental data can be misinterpreted and gross design errors can be made. For instance, we have shown⁷ that for binary systems in the literature, there are instances where data is reported as solid-fluid equilibrium but the equation-of-state model, with parameters regressed by the authors from their experimental data, actually predicts vapor-liquid equilibrium (VLE). This generally occurs because the researchers assume that the model will predict solid-fluid equilibrium and either do not check for phase stability or do the phase stability check using a local solution technique that does not guarantee the correct solution. In some cases, authors have

recognized that their experimental data seemed suspicious (i.e., solubilities too high for the solid dissolved in a supercritical fluid phase) and they later verified that what they had originally believed to be solid-fluid equilibrium was really vapor-liquid equilibrium, in agreement with the model predictions.^{8,9} As we will discuss here, the likelihood of such errors greatly increases when one computes high-pressure phase equilibria involving solids in *multicomponent* mixtures using conventional numerical solution techniques.

There are a wide variety of industrial processes where correct modeling of solid-fluid equilibrium is important. The most obvious are those involving supercritical fluid extraction, which has found extensive application for coffee and tea decaffeination, and for the recovery of components in natural products, such as hops, essential oils and nutraceuticals.¹ A common practice is to add a chemical modifier (called a cosolvent or entrainer) to the supercritical fluid in order to increase solute solubility or selectivity. For instance, a polar cosolvent such as ethanol might be added to nonpolar supercritical CO₂ to increase the solubility of polar compounds. As a result, most supercritical fluid extractions involve multicomponent mixtures. Moreover, there is a large body of data in the literature on the solubility of solid solutes in supercritical fluids that have been modified with the addition of either gaseous or liquid cosolvents.^{10,11,12,13} In particular, the practice of adding cosolvents has been used extensively with supercritical carbon dioxide, which has a relatively low solvent power, but which is used frequently since it is inexpensive and environmentally benign. A supercritical extraction process with a cosolvent usually begins by first mixing a certain proportion of the cosolvent and solvent at a particular temperature and pressure that ensures that a single phase exists, i.e., above the mixture critical point of the binary solvent-cosolvent system. Then this mixture is passed to another unit to contact the solid and extract the solute. In modeling the solubility of the solute in the extraction,

the solvent to cosolvent ratio is fixed, and then one solves for the solubility that satisfies the equifugacity requirement of the solute in both the solid and supercritical phases. It is customary to neglect the possibility of a second fluid phase (liquid) forming (fluid phase instability) in both measurement and modeling as long as the original solvent-cosolvent mixture remains above its binary mixture critical point. However, as we will demonstrate here, this can lead to erroneous results.

A second type of application in which reliable modeling of high-pressure, multicomponent phase behavior involving a solid phase is important is materials production using the RESS, GAS or SAS processes. For instance, the point at which a solid precipitates from a liquid with the addition of a pressurized gas forms the basis of the gas anti-solvent process (GAS) and supercritical anti-solvent process (SAS). Therefore, these processes invariably require knowledge of the multicomponent saturation conditions for adequate development. A third type of application of interest in this context is the use of supercritical fluids as solvents for reactions. Many reactions in supercritical fluids involve the presence of both solid and liquid reactants, products, and catalysts, and reliable computation of phase behavior is important because frequently single phase operation is desired. For a review of homogeneous reactions in supercritical fluids see Jessop *et al.*¹⁴

We will present here a completely reliable computational strategy, based on interval analysis, to find the solution to high-pressure, multicomponent phase equilibrium problems involving a solid phase. The examples given are for solid-fluid equilibrium in the presence of cosolvents, as might be encountered in a supercritical fluid extraction process, but this computational technique can also easily be used in modeling the phase behavior in the other high-pressure phase equilibrium applications mentioned above. First, we will present a brief

overview of the features of high-pressure solid-fluid phase behavior, in order to illustrate the inherent complexity that can be encountered in modeling these systems. Then we will detail the problem formulation and summarize the solution method based on interval analysis. Finally, we will give several examples in which we have applied this technique. These are taken from the literature, and illustrate the importance of reliable computation of high-pressure phase equilibrium for multicomponent mixtures with solids present.

2. BACKGROUND

In this section, we will present a brief overview of the features of high-pressure solid-fluid phase behavior, and discuss some of the modeling difficulties that can result.

2.1 Binary Phase Behavior

It has been known for some time that solid solutes can undergo melting below their normal melting points with an increase in pressure of a compressed gas.^{15,16,17} For binary systems with a temperature specified in an appropriate range, there is one (or possibly more than one) value of pressure at which the solid melts to form a three phase, solid-liquid-vapor (SLV) system. This is shown in Figure 1, which is a pressure-temperature (PT) projection of a typical asymmetric system, such as naphthalene and ethane.¹⁸ Most supercritical fluid extraction systems are designed to operate at temperatures between the two SLV regions, usually above the lower critical end-point (LCEP) and below the upper critical end-point (UCEP). The critical end-points are where two phases become identical in the presence of a third phase; e.g., vapor and liquid become critical in the presence of a solid phase. Above the sublimation pressure of the solid, only equilibrium between two phases (either solid-vapor or solid-supercritical fluid equilibrium) can exist at temperatures and pressures between the LCEP and UCEP, except for the case with a temperature minimum in the SLV curve, as shown by curve II in Figure 1 (which

will be discussed below). At temperatures close to the UCEP or LCEP one can observe large changes in solvent power with small changes in pressure.¹⁹ If the temperature is above the UCEP (or above the minimum in the SLV curve, as discussed below), the solid will melt and one will observe VLE, unless a large loading of the solid solute is used, which will result in solid-liquid equilibrium (SLE). If the pressure is further increased, the liquid and vapor phases will disappear at the mixture critical point and either a single phase will exist or one will observe SFE at large solute loadings. The upper (higher temperature) SLV line emanates from the solute triple point and proceeds directly to the UCEP as illustrated as SLV curve I in Figure 1. However, for some systems, *e.g.* naphthalene and CO₂,⁹ and biphenyl and CO₂,⁹ the SLV line proceeds through a minimum in temperature (SLV curve II in Figure 1) before reaching the UCEP. For these systems, simply remaining below the UCEP temperature does not guarantee working in a SFE region; one must be below the minimum in the SLV curve.

Cubic equations of state (EOS) can describe all of the types of phase behavior mentioned above. However, we have shown previously that there can exist multiple solubility roots to the equifugacity equations for solid-fluid equilibrium when using cubic EOS at temperatures near the SLV lines.⁷ The key to identifying the correct root(s), and, thus, the correct type of phase equilibrium (SFE, SLE or SLV), is testing the roots for thermodynamic stability. If there is no solubility root that is both stable and feasible (based on overall solute loading and material balance), then there is no solid phase present at equilibrium, and a multiphase flash calculation can be done to determine the number and composition of fluid phases present. Xu *et al.*⁷ demonstrate that their solution strategy can correctly deal with all these cases, thus determining the correct behavior. This is extremely useful in modeling experimental data to ensure that one does not regress parameters that predict the existence of phases that are not observed

experimentally. This is also important in alerting experimentalists *a priori* to the possibility of unanticipated phase transitions. Obviously, *a priori* predictions are only as good as the models (and interaction parameters) employed, but they can at least qualitatively indicate the phase behavior to be expected. Whether one assumes SFE, or includes the possible existence of liquid phases,^{20,21,22} and whether there are single or multiple roots to the equifugacity equation, the key step in computing the correct phase behavior is performing a completely reliable phase stability test. This is all the more important for the high-pressure multicomponent case, as discussed next.

2.2 Ternary Phase Behavior

In ternary mixtures, as occurs when a cosolvent is added to a supercritical fluid to enhance the solubility or selectivity of a solid solute, the possibility of liquid phase formation is greatly enhanced in comparison to the binary case. According to the Gibbs phase rule, a third component extends SLV equilibrium from a *line* to a *region* of pressure and solubility at a given temperature. This is represented in Figure 2, which shows a typical scenario encountered when a gaseous or liquid cosolvent is added to a supercritical fluid at a certain initial concentration. At low pressures, P_A in Figure 2, solid-vapor (SVE) equilibrium exists, with the solute solubility (mole fraction) y_2 in the vapor shown by the solid curve, assuming an overall solute loading of at least y_2 (otherwise there will be a single vapor phase mixture). As pressure is increased, the SLV region is encountered, bounded at its lowest pressure by the first melting line, and at its highest pressure by the first freezing line. In this region, P_B in Figure 2, if there is a sufficiently large solute loading, then there is SLV equilibrium. At lower solute loadings, VLE would exist, and at still lower solute loadings, a single vapor phase mixture would exist. If the solute loading is such that VLE occurs, then the compositions of the liquid and vapor phases depend on the loading. This is shown in the figure by the three different curves at low, “critical” and high loadings, ψ_{low}

$< \psi_{\text{crit}} < \psi_{\text{high}}$. Only at one particular loading, designated ψ_{crit} , does the curve close at higher pressure. At the other loadings, the overall mixture composition point is simply no longer in the VLE region as the pressure is increased (note that Figure 2 is a two-dimensional representation of a three component system). Beyond the SLV region, P_C in Figure 2, one can observe SLE, single-phase liquid, VLE, or single-phase vapor, depending on the solute loading. If SLE exists (high solute loading) then the liquid phase composition (solute solubility) is given by the solid line at high mole fraction. At high pressures, P_D in Figure 2, SLE exists for high solid loadings; at lower loadings one would observe a single fluid phase.

The phase behavior explained above can be further visualized using the triangular ternary phase diagrams in Figures 3-6, corresponding to the pressures P_A , P_B , P_C and P_D shown schematically in Figure 2. Although certainly not to scale, the reader might think of the system as being naphthalene (solute) and CO_2 (solvent), where propane has been added as a cosolvent. On each plot, there is a dashed straight line that extends from the pure naphthalene vertex to the CO_2 /propane edge of the triangle. This line represents a constant solvent/cosolvent loading, as one would encounter with a premixed CO_2 /propane mixture, such as that used by Smith and Wormald.¹⁸ The position of the initial overall composition point along that straight line depends on how much solute (naphthalene) is loaded.

Figure 3 illustrates the low-pressure condition, P_A from Figure 2. Each of the sides of the triangle represents the conditions if the third component were absent: SLE for naphthalene and propane (assuming that P_A is greater than the vapor pressure of propane), SVE for naphthalene and CO_2 , and a single phase for CO_2 and propane (which assumes that the pressure is above the mixture critical point of this binary). Since the constant solvent/cosolvent ratio line only passes through the SV equilibrium and single-phase vapor sections of the diagram, these are the only

types of phase behavior that can exist at this pressure. There will be a single vapor phase if the solute loading is very low, and SVE if the solute loading is high enough to put the overall mixture composition point into the SV region. If the cosolvent to solvent ratio were to be increased, thus shifting the constant solvent/cosolvent ratio line to the right, then one might observe other kinds of phase behavior, including SLV, VLE, SLE, single-phase liquid or single-phase vapor, depending on the solute loading.

Figure 4 illustrates pressure P_B , which cuts through the SLV region in Figure 2. SLV equilibrium is found within a triangular region where the compositions of the phases are found at the vertices of the SLV triangle, which includes pure solid naphthalene. At high solute loadings (anywhere within the SLV triangle) SLV equilibrium occurs, while at smaller solute loadings along the constant solvent/cosolvent ratio line, VLE is encountered. Note that, even though there is an overall constant solvent/cosolvent ratio, in SLV and VLE the solvent/cosolvent ratio in each phase is different. From this diagram it is also easy to see why the vapor and liquid compositions in VLE depends on the solute loading, as this determines the tie line representing the equilibrium.

A common feature of Figures 3-6 is the “S” shaped curve that extends from the naphthalene/propane side of the triangle to the naphthalene/CO₂ side. Notice its movement towards the naphthalene/CO₂ side with an increase in pressure, as seen from Figure 3 to Figure 6. As the “S” shaped curve (and its associated phase equilibrium features) moves towards the naphthalene/CO₂ side the constant solvent/cosolvent ratio line passes through increasingly more complex phase behavior, as shown by the triangular diagram for pressure P_C in Figure 5. For the solvent/cosolvent ratio shown by the straight dashed line, one can observe SLE, single-phase liquid, VLE, or single-phase vapor, depending on the solute loading. Note that the phase

behavior would be SVE if the propane cosolvent were not present. However, with the propane present there is the possibility of liquid phase formation. From Figure 5 it is also easy to see why some of the VLE curves in Figure 2 terminate. For example, one can identify loadings on the constant solvent/cosolvent ratio line that were in the VLE envelope in Figure 4 but that are in the single phase liquid region in Figure 5. Thus, the VLE envelope of these loadings would “terminate” at a pressure between P_B and P_C , as shown by ψ_{high} in Figure 2.

As shown in Figure 6 (neglecting box *a* for now), with a further increase in pressure to P_D the constant solvent/cosolvent ratio line no longer intersects the VLE envelope, and there remains only one dense liquid-like state for SFE at high solute loading, and a single fluid phase at lower solute loading. However, if the temperature of the system is changed to above the binary SLV line of the naphthalene/ CO_2 system, then a VLE dome will appear emanating from the naphthalene/ CO_2 side of the triangle, as shown in box *a* in Figure 6.

Thus, ternary and higher multicomponent systems exhibit many possibilities for complex phase behavior, including the formation of liquid phases. As a result, there is a strong need for reliable techniques to compute the high-pressure phase behavior of such systems. We will demonstrate here a technique based on interval analysis that can provide a *guarantee* that the phase equilibrium computations give correct results.

3. PROBLEM FORMULATION

To solve the phase equilibrium problem, it is first assumed that there is solid-fluid equilibrium and then the corresponding equifugacity conditions are solved for *all* roots. The roots are then tested using tangent plane analysis to determine if any represents a stable phase equilibrium state. If no stable roots are found, then this indicates that at the specified temperature, pressure, and overall composition, there is no solid-fluid equilibrium. In this case,

the problem is treated as a general multiple-fluid-phase flash with possible solid phase. In this section, we summarize the formulation of each of these parts of the overall computation.

3.1 Equifugacity Conditions

The formulation used for the equifugacity conditions is developed in detail by Xu *et al.*⁷, and is summarized briefly here. The species in the multicomponent system are designated as solvent (component 1), solute (component 2), and cosolvent (components 3, 4, ..., C). Assuming a pure solid solute phase in equilibrium with a single fluid phase containing all components, then the equifugacity conditions are:

$$f_2^S(T, P) = \hat{f}_2^F(T, P, v, \mathbf{y}) \quad (1)$$

$$\sum_{i=1}^C y_i = 1 \quad (2)$$

$$P = \mathfrak{Z}_P(T, v, \mathbf{y}) = \frac{RT}{v - b_m(\mathbf{y})} - \frac{a_m(T, \mathbf{y})}{v(v + b_m(\mathbf{y})) + b_m(\mathbf{y})(v - b_m(\mathbf{y}))} \quad (3)$$

$$y_1 = \alpha_i y_i, \quad i = 3, \dots, C. \quad (4)$$

Here Eq. (1) is the equifugacity equation for the solute, with f_2^S indicating the fugacity of the solute in the pure solid phase, \hat{f}_2^F the fugacity of the solute in the fluid-phase solution, v the molar volume of the fluid phase, and $\mathbf{y} = (y_1, y_2, \dots, y_C)^T$ the vector of fluid-phase mole fractions. Equation (3) is the equation of state (EOS) for the fluid phase, and indicates the use of the Peng-Robinson (PR) EOS. Here a_m and b_m are the mixture attractive energy and co-volume parameters of the PR EOS, and these are determined using standard (van der Waals) mixing rules. Equation (4) specifies the molar solvent to cosolvent ratios α_i for each cosolvent. The

ratios α_i are specified, as are the system temperature T and pressure P . Equations (1-4) thus represent a system of $C+1$ equations that can be solved for the $C+1$ variables \mathbf{y} and v . Once \mathbf{y} has been determined, the molar phase fraction β^S of the solid phase can be determined from the solute material balance

$$\beta^S + y_2(1 - \beta^S) = \psi_2, \quad (5)$$

where ψ_2 is the specified overall mole fraction of solute (overall solute loading). In solving Eqs. (1-4) it is important to realize that there may be multiple solutions. To ensure that the phase equilibrium problem is correctly solved, it is necessary to find *all* the equifugacity roots. A solution method, based on interval mathematics, that can deal rigorously with the issue of multiple solutions is discussed below.

There are alternative methods for determining the pure solid phase fugacity f_2^S , based on the type of physical property data that is available. In the examples below, unless otherwise noted, an expression based on sublimation pressure data is used:

$$f_2^S(T, P) = P_2^{\text{sub}}(T) \exp\left[\frac{v_2^S(P - P_2^{\text{sub}}(T))}{RT}\right]. \quad (6)$$

Here P_2^{sub} is the solute sublimation pressure and v_2^S is the molar volume of the pure solid (assumed constant). An alternative expression¹⁸, used in some cases for consistency in making comparisons to the literature, is

$$\ln\left[\frac{f_2^S(T, P)}{f_2^L(T, P, v^L)}\right] = \frac{\Delta h_2^{\text{fus}}}{R} \left(\frac{1}{T_m} - \frac{1}{T}\right) - \int_{P_2^{\text{sub}}(T)}^P \frac{v^L(T, P) - v^S}{RT} dP \quad (7)$$

Here f_2^L and v^L refer to a hypothetical subcooled pure liquid solute and are based on the fluid-phase EOS, and Δh_2^{fus} and T_m are the experimental molar heat of fusion and normal melting temperature.

3.2 Stability Analysis

Solutions to the equifugacity conditions may represent stable, metastable or unstable states. Since carefully measured equilibrium data most likely represent thermodynamically stable data, it is desirable to deal exclusively with stable computational results. For this purpose, tangent plane analysis²³ is widely used. A fluid phase of composition (mole fraction) \mathbf{y}_0 is not stable (i.e., unstable or metastable) if the Gibbs energy vs. composition surface ever falls below a (hyper)plane tangent to the surface at \mathbf{y}_0 . The Gibbs energy surface here consists of two parts, one corresponding to the fluid phase (or phases), and another corresponding to the solid phase. For the fluid case, we will express the Gibbs energy surface using $g_m(\mathbf{y},v)$, the (molar) Gibbs energy of mixing (i.e., the Gibbs energy relative to pure component fluids at the system temperature and pressure). Here v and g_m are determined using the fluid-phase EOS; if there are multiple volume roots, then the one yielding the smallest value of g_m must be used. For the solid case, since a solid phase is assumed to consist of pure solute, its part of the Gibbs energy vs. composition surface consists of only a single point, which lies on the pure solute axis. Relative to pure *fluid* solute at the system temperature and pressure (to be consistent with the reference state used for the fluid-phase surface g_m), this point has a (molar) Gibbs energy value

$$g_2^S = RT \ln \left(\frac{f_2^S}{f_2^F} \right) \quad (8)$$

Here f_2^S is determined from either Eq. (6) or (7), and f_2^F is computed using the EOS with $y_2 = 1$. This representation of the Gibbs energy surface is discussed in much more detail by Xu *et al.*⁷ and Marcilla *et al.*²⁴

The distance between the Gibbs energy surface and the tangent plane is referred to as the tangent plane distance. A plane tangent to the Gibbs energy surface at the fluid phase

composition \mathbf{y}_0 is given by

$$g_m^{\text{tan}}(\mathbf{y}) = g_m(\mathbf{y}_0, v_0) + \sum_{i=1}^c \left(\frac{\partial g_m}{\partial y_i} \right)_{\mathbf{y}_0} (y_i - y_{i,0}). \quad (9)$$

Relative to the fluid phase Gibbs energy surface, the tangent plane distance is then

$$D^{\text{F}}(\mathbf{y}, v) = g_m(\mathbf{y}, v) - g_m^{\text{tan}}(\mathbf{y}) \quad (10)$$

and relative to the solid phase it is

$$D^{\text{S}} = g_2^{\text{S}} - g_m^{\text{tan}}(y_2 = 1) \quad (11)$$

If D^{F} is negative for any value of \mathbf{y} , or if D^{S} is negative, then this indicates that the Gibbs energy surface is below the tangent plane and thus the phase of composition \mathbf{y}_0 being tested is not stable.

If \mathbf{y}_0 is a solution to the equifugacity conditions for solid-fluid equilibrium, then the tangent plane will pass through g_2^{S} (see Xu *et al.*⁷ and Marcilla *et al.*²⁴ for discussion) and thus D^{S} is zero. Otherwise, the sign of D^{S} can be checked by a straightforward point evaluation. To determine if D^{F} ever becomes negative is a much more challenging problem. This is typically done by seeking the minimum of D^{F} with respect to \mathbf{y} by finding its stationary points in the space constrained by the y_i summing to one. However, it is common for there to be multiple local minima in D^{F} , and thus it is critical that the *global* minimum be found. If the global minimum of D^{F} is negative, then the phase being tested is not stable; otherwise it is stable. While only the global minimum needs to be found for purposes of the stability analysis, it is in fact useful to find the other stationary points as well, since as noted below, when the phase being tested is not stable, the stationary points are useful in initializing subsequent phase split computations. A solution method, again based on interval mathematics, that can deal rigorously

(deterministically) with the issue of the global minimization, as well as finding all the stationary points, is discussed below.

3.3 Multiple-Fluid-Phase Flash with Possible Solid Phase

If it is determined that there are no solutions of the equifugacity conditions for solid-fluid equilibrium that correspond to a stable equilibrium state, then there is no solid-fluid equilibrium at the specified temperature, pressure, and overall composition. In this case, the problem is now treated as a general multiple-fluid-phase flash with a possible solid phase. There are now many flash algorithms for multi-fluid-phase equilibrium, of which the algorithm of Lucia *et al.*²⁵ is especially reliable (though not guaranteed). However, there are few flash algorithms for the case of multiple fluid phases in equilibrium with a solid phase at high-pressures, using an EOS model for the fluid phases; see Zhou *et al.*²⁶ for example.

The method used here is a two-stage approach that alternates between phase split and phase stability calculations. In the phase split problem, the number of fluid phases and whether or not a solid phase is present is first postulated, generally based on information from a preceding phase stability analysis, and then the corresponding Gibbs energy minimization problem is solved for a potential equilibrium state. If there are NP fluid phases, labeled I, II, ..., NP , and a pure solid solute phase, labeled S, then the minimization problem is:

$$\min \left\{ \beta^I g_m^I(\mathbf{y}^I, v^I) + \beta^{II} g_m^{II}(\mathbf{y}^{II}, v^{II}) + \dots + \beta^{NP} g_m^{NP}(\mathbf{y}^{NP}, v^{NP}) + \beta^S g_2^S \right\} \quad (12)$$

subject to the mole fractions summing to one in each phase, the EOS in each phase, and the overall material balance

$$\beta^I + \beta^{II} + \dots + \beta^{NP} + \beta^S = 1 \quad (13)$$

$$\beta^I y_i^I + \beta^{II} y_i^{II} + \dots + \beta^{NP} y_i^{NP} + \beta^S y_i^S = z_i, \quad i = 1, 2, \dots, C-1, \quad (14)$$

where β^j is the molar phase fraction for phase j and z_i indicates the overall mole fraction of species i . Note that $y_2^S = 1$ and that $y_i^S = 0, i \neq 2$, since the solid phase is pure solute. For the solute, z_2 equals ψ_2 , the specified fractional loading of solute in the system being studied. For the solvent and cosolvents, the z_i are readily determined from the specified solvent to cosolvent ratios α_i together with the summation of the z_i to one. In solving this optimization problem, one needs to find only a local minimum, since if the global optimum is not found, this will be detected in the subsequent phase stability analysis, which in effect is a global optimality test. Good initial guesses for the local optimization can generally be obtained by using stationary points from the preceding stability analysis. For solving this optimization problem, we use the successive quadratic programming (SQP) approach described and implemented by Chen and Stadtherr.²⁷ However, there are many other approaches that could be used to perform this local optimization, and that may perform better than SQP in this context. Furthermore, there are alternative problem formulations that could be used; for example, the use of mole numbers rather than mole fractions as independent variables. It is not critical in the phase split computation what approach is used, as long as it converges to a local minimum in the Gibbs energy.

Once a potential equilibrium state is found by locating a minimum in the optimization problem, then it is tested using phase stability analysis, as described above. If this indicates that the state is not stable, then either 1) the phase-split optimization problem is solved again with the same number and type of phases, but with new initial guesses based on the newly found stationary points, or 2) the phase-split optimization problem is reformulated by adding a new phase. This type of two-stage strategy that alternates between phase split and phase stability calculations is widely used for the case in which there are fluid phases only^{25,28,29}, and can be

shown³⁰ to converge in a finite number of steps to the equilibrium solution, provided that the phase stability problem is solved to global optimality.

4. SOLUTION METHODOLOGY

To correctly solve the problems formulated above, it is necessary to have a procedure that is capable of reliably locating *all* the solutions of a nonlinear equation system and to have a deterministic procedure that is capable of locating the *global* optimum of a nonlinear function. These capabilities can be provided through the use of interval analysis.

4.1 Interval Analysis

Good introductions to interval analysis, as well as to interval arithmetic and computing with intervals, include those of Neumaier³¹, Hansen³² and Kearfott.³³ Of particular interest here is the interval-Newton/generalized bisection (IN/GB) technique. Given a nonlinear equation system with a finite number of real roots in some specified initial interval, this technique provides the capability to find (or, more precisely, to enclose within a very narrow interval) *all* the roots of the system within the given initial interval. This can be applied directly to the solution of the equifugacity conditions, as formulated above. To apply this technique to the minimization problem of interest in phase stability analysis, IN/GB is used to solve a nonlinear equation system for *all* the stationary points in the optimization problem. Alternatively, this can be done in combination with a simple branch-and-bound scheme, so that all the stationary points do not need to be found, only the one corresponding to the global minimum. However, as noted above, knowledge of the stationary points may be useful for initializing the phase split computations, so we typically use IN/GB to find all the stationary points. These procedures are

outlined in more detail by Xu *et al.*⁷, and further details are given by Hua *et al.*^{34,35} and Schnepfer and Stadtherr.³⁶

Properly implemented, the IN/GB technique provides the power to find, *with mathematical and computational certainty*, enclosures of *all* solutions of a system of nonlinear equations, or to determine *with certainty* that there are none, provided that initial upper and lower bounds are available for all variables.^{31,33} This is made possible through the use of the powerful existence and uniqueness test provided by the interval-Newton method. The technique can also be used to enclose *with certainty* the *global* minimum of a nonlinear objective function³², again assuming an initial interval is provided for all variables. Note that unlike standard *local* equation-solving and optimization routines, which require a point initialization, the IN/GB approach requires only an initial *interval*. Since this initial interval can be made sufficiently large to include all physically feasible possibilities, this makes the methodology essentially initialization independent. The interval methodology has been successfully applied to solve a wide variety of thermodynamic phase behavior problems.^{7,37,38} The overall strategy for solving the phase behavior problem of interest here is outlined below.

4.2 Problem-Solving Strategy

It is first assumed that there is solid-fluid equilibrium, so the equifugacity conditions, Eqs. (1-4), are solved using the interval methodology. From Eq. (5), it is clear that $0 \leq y_2 \leq \psi_2$, thus the initial interval for y_2 is $[0, \psi_2]$. Initial intervals for the remaining fluid-phase mole fractions y_i can then be determined from Eqs. (2) and (4), using interval arithmetic and the initial interval for y_2 . In the initial interval for v , the lower bound is taken to be the smallest of the pure component co-volume parameters, that is, $\min_i b_i$, and the upper bound is taken to be $2RT/P$

(compressibility factor of 2). Application of the IN/GB approach will now determine all roots, if any, within these initial intervals.

One possibility is that there could be one or more equifugacity roots. In this case, each root is tested for phase stability as described above, using the interval methodology to assure correct results. For solving the phase stability problem, each mole fraction y_i has the initial interval $[0, 1]$, and the initial volume interval is the same as used in solving the equifugacity condition. If there is a root that tests stable, then a solid-fluid equilibrium state has been found. It is also possible that more than one equifugacity root will test as stable; this indicates an equilibrium state with a solid phase and multiple fluid phases (corresponding to the multiple stable equifugacity roots). If none of the roots test as stable then there is no solid-fluid equilibrium state. In this case, we postulate two fluid phases plus a solid phase, and initiate the two-stage procedure described in section 3.3 that alternates between phase split and phase stability calculations until the correct number and type of phases and phase compositions are found. The result will be multiple-fluid-phase equilibrium that may or may not include a solid phase. The procedure used is a modification of the INTFLASH routine described by Hua³⁹ and also applied by Stradi *et al.*⁴⁰ and Xu *et al.*⁷ The original INTFLASH performs multiple-fluid-phase flash calculations; the modification accounts for the possibility of a pure solid phase also present.

Alternatively, another possibility is that there could be no equifugacity roots. This indicates that the solute loading ψ_2 was sufficiently small that all the solid dissolved. Thus, a single fluid phase with $y_2 = \psi_2$ is next postulated, and this is tested for phase stability as described above. If the test indicates stability, then the equilibrium state is a single fluid phase with $y_2 = \psi_2$; otherwise two fluid phases are next postulated, and we again initiate the two-stage

procedure described in section 3.3 that alternates between phase split and phase stability calculations until the correct number of phases and phase compositions are found.

5. RESULTS AND DISCUSSION

5.1 Example 1: Naphthalene and CO₂ with Gaseous Cosolvents Ethane and Propane

The solubility of naphthalene in the solvent/cosolvent mixtures CO₂/C₂H₆ and CO₂/C₃H₈ has been investigated by Smith and Wormald.¹⁸ Both systems were measured at temperatures from 35 °C to 60 °C, and at pressures from 60 to 250 bar. They also determined the SLV equilibrium (first melting line) for these systems, and modeled the data using the Peng-Robinson EOS with van der Waals mixing rules. Their model computations were based on the equifugacity condition, using Eq. (7) for the solid fugacity, but without stability analysis. For their model, they took values of the binary interaction parameters k_{12} and k_{13} from the literature, and fit values of k_{23} to their experimental solubility versus pressure data. Exactly the same model is used for the computations done in this example. The binary interaction parameter values¹⁸ used are $k_{12} = 0.090$, $k_{13} = 0.131$ (3 = ethane), $k_{13} = 0.125$ (3 = propane), $k_{23} = 0.040$ (3 = ethane) and $k_{23} = 0.041$ (3 = propane). Other physical property data used in the model are given in Table 1.

Using the strategy described in Section 4.2, the solubility y_2 of naphthalene in CO₂/C₂H₆ ($\alpha_3 = 0.7$) and CO₂/C₃H₈ ($\alpha_3 = 5.6$) was computed at several temperatures over a pressure range that includes the range studied by Smith and Wormald. Figure 7 shows the computed results for CO₂/C₂H₆ at $T = 307.9$ K, along with the data of Smith and Wormald¹⁸. As shown, at each pressure there is a single solubility root to the equifugacity condition, which was confirmed to be stable using the interval method. Figure 8 shows the results for $T = 323$ K. Here there is a large

range of pressure for which there are three equifugacity roots. The roots representing stable equilibrium are denoted by the solid curve. At lower pressures (below about 100 bar), the smallest solubility root is stable, implying solid-vapor equilibrium. Then, according to Smith and Wormald's model¹⁸, around 100 bar, a very small region (which appears in Figure 8 as a heavy vertical line) of SLV equilibrium appears, bounded by the first melting and last freezing pressures. In this pressure region, Smith and Wormald's model¹⁸ indicates that large solute loadings result in SLV equilibrium, *i.e.*, liquid phase formation, and at lower loadings VLE exists, with phase compositions determined by the solute loading (see Section 2.2). At pressures above the SLV region, the highest solubility root is stable, implying solid-liquid equilibrium provided that the solute loading is sufficient. At lower solute loadings there can be VLE with the phase compositions varying according to the loading. In Figure 8, the VLE region is shown as a dashed-dotted line for the case of a near critical loading. Figure 9 shows the results for $T = 333$ K for the Smith and Wormald model¹⁸, which are qualitatively similar to the 323 K case. Here the SLV region is again very narrow, from about 61.75 to 62.25 bar. Clearly, for the situations depicted in Figures 8 and 9, reliable stability analysis is critical in determining the nature of the phase behavior predicted by the model.

For the 323 K and 333 K cases (Figures 8 and 9) there is a discrepancy between the SFE data of Smith and Wormald¹⁸ and the stable SFE predicted by their model. In other words, there is an inconsistency between Smith and Wormald's reported experimental data and their model.¹⁸ This means one of two things. One possibility is that the model is simply inadequate. This could be due to a fundamental inability of the simple Peng-Robinson equation to model this system, or, perhaps, it could be due to a significant temperature dependence of one or more of the binary interaction parameters that is not taken into account. Another possibility is that the experimental

SFE results reported are not really SFE. We have some additional insight into this system because Smith and Wormald¹⁸ also measured the SLV equilibrium (first melting curves). Interestingly, the experimental SLV lines that Smith and Wormald¹⁸ report confirm that portions of their SFE data actually reside inside the VLE region, similar to the results obtained by their model. However, since the measurements were taken in a flow apparatus, they may not be meaningful VLE data. For ternary systems, VLE is dependent on the overall loading of the components, with different loadings producing different compositions in each phase. Thus for VLE data to be meaningful, the overall composition it corresponds to must be known. However, in a flow system the loadings are constantly changing, and so in principle the overall composition is not known. In practice it may be that the loadings will undergo only insignificant changes, though, if so, this should be determined *a priori*.

Figures 10 and 11 show the results for the case of propane as cosolvent with $\alpha_3 = 5.6$. At $T = 308.3$ K, as shown in Figure 10, there is a single stable solubility root to the equifugacity condition, similar to the situation in Figure 7 for the ethane cosolvent. At $T = 328.3$ K, as shown in Figure 11, there are multiple equifugacity roots, and the situation is similar to that shown in Figures 8 and 9 for the ethane cosolvent. In this case, however, the SLV region is much wider, ranging from about 62 to 78 bar, due to the fact that CO₂ and propane are chemically less similar than CO₂ and ethane. Again, there is an inconsistency between the data and the model used by Smith and Wormald.¹⁸ Either the model is totally inadequate or the experimental phase equilibrium has been misidentified. If the latter is the case, then it would mean that the experimental data reported as SFE by Smith and Wormald¹⁸ might actually be VLE which is predicted by their model, assuming an appropriate solute loading.

5.2 Example 2: Naproxen and CO₂ with a Liquid Cosolvent

The solubility of naproxen in supercritical CO₂ with various cosolvents was measured and modeled by Ting *et al.*⁴¹ They studied the cosolvents acetone, ethyl acetate, methanol, ethanol, 1-propanol and 2-propanol. These cosolvents are liquids at ambient conditions and are different than the nonpolar gases that served as cosolvents in the previous example. The presence of a highly asymmetric cosolvent (whose polarity and critical properties are very different than those of CO₂) provides for even richer phase behavior than that shown schematically in Figures 2-6. Due to the possible association between the cosolvent and the solute, naproxen, the experimental solubility enhancement was considerable compared with the cosolvent-free case. They qualitatively represent the solubility enhancement by using the concept of the *cosolvent effect*, which is defined as the ratio of the solubility obtained with the cosolvent to that obtained without cosolvent at the same temperature and pressure. It was demonstrated that the cosolvent effect (increase in solubility with the cosolvent) increases in the order ethyl acetate, acetone, methanol, ethanol, 2-propanol and 1-propanol.

Ting *et al.*⁴¹ believed that no liquid phase formed throughout their experiments, substantiated by no evident melting in their samples after depressurization. Therefore, they assumed a solid-fluid equilibrium model and then regressed interaction parameters for the Peng-Robinson EOS with van der Waals mixing rules. As discussed above, if two-phase solid-fluid is the true equilibrium state, then the fluid phase itself must be thermodynamically stable. However, using the procedure for stability analysis described above demonstrates that this is not true for all temperatures and pressures investigated. In other words, there is an inconsistency or mismatch between the data and the model presented by Ting *et al.*⁴¹ As described in Example 1, this means one of two things. One possibility is that the model presented by Ting *et al.*⁴¹ is

inadequate, i.e., it is not able to describe the real phase behavior with the parameters they used. A second possibility is that the experimental data, which was presented as SFE, was actually not SFE.

As a specific example, consider the case of acetone as cosolvent ($\alpha_3 = 96.5/3.5$) at $T = 333.1$ K. Using the binary interaction parameter values $k_{12} = 0.229$, $k_{13} = 0$ and $k_{23} = -0.196$ regressed by Ting *et al.*⁴¹, the physical property values estimated by Ting *et al.*⁴¹ (see Table 1), and the computational procedure given above, the true equilibrium state predicted by the Peng-Robinson EOS with van der Waals mixing rules has multiple fluid phases, except at the two highest pressures considered (165.5 and 179.3 bar). Table 2 shows results for the case in which the initial solute loading is $\psi_2 = 0.25$, which is sufficiently high to give SLV equilibrium. If the solute loading is lower, the results are VLE (except at 165.5 and 179.3 bar), with the phase compositions dependant on the specific solute loading. The experimental data, identified by Ting *et al.*⁴¹ as solid-fluid equilibrium, are also listed for comparison. The fact that the experimental solubilities are fairly close to the computed solubilities for the SLV case, suggests that experimentally there might have been a liquid phase present. If experimental SLV data were available, better interaction parameters values could then be regressed from this data. If in fact there was small amount of liquid phase present in the experimental measurements, then this could have a significant impact on the physical interpretation of the cosolvent effect, since the concentration of solute in this phase is quite high. While we have focused in this example on the acetone cosolvent case, the same issue (model predicts that the fluid phase is not stable) occurs with the other cosolvents studied as well.

One can learn from this example that, without reliable computation of phase stability, experimental data may end up being fit to an unstable solution of a thermodynamic model, thus

leading to misinterpretation of both experimental and modeling results. The investigators of this system inferred from their observations that there was no liquid phase present, though liquid phase formation might be difficult to observe due to the small liquid phase fraction and insufficient equilibration time for melting. With the current parameters, this model predicts SLV equilibrium, not SFE as the modelers intended. This suggests the need for further studies into this cosolvent system in a static high-pressure view cell to ascertain its true phase behavior. Once determined, interaction parameters that predict the true stable equilibrium could be regressed, which would lend greater confidence to process design and simulation.

5.3 Example 3: β -Naphthol and CO₂ with Methanol Cosolvent

The system of β -naphthol/CO₂ with a methanol cosolvent was investigated by Dobbs *et al.*,⁴² Dobbs and Johnston,⁴³ and Lemert and Johnston.⁴⁴ The solubility of β -naphthol in CO₂ mixtures with as much as 9.0 mole % methanol were measured by Dobbs and Johnston⁴³, and SLV equilibrium was measured and modeled by Lemert and Johnston⁴⁴ up to 4.0 mole % methanol. Lemert and Johnston⁴⁴ calculated the SLV equilibrium (“first melting” line) by specifying the pressure and determining the lowest temperature yielding SLV equilibrium. In other words, for a given pressure and solvent/cosolvent ratio, the system is a solid phase in equilibrium with a single vapor or fluid phase until the temperature is raised high enough to cause melting; this is the temperature corresponding to the “first melting” line found by Lemert and Johnston.⁴⁴ Especially when cosolvents are present, this SLV line can be significantly below the normal melting point of the solid. The SLV line was computed from the equifugacity relationship using the Peng-Robinson equation of state for the vapor phase, Regular Solution Theory for the liquid phase fugacity, Eq. (7) for the solid phase, and the physical property data given in Table 1. The experimental SLV equilibrium and the model agreed well.

The computational procedure that we have described above can also be used to detect the SLV equilibrium (“first melting” line) in a typical extraction situation, such as this, that involves cosolvents. Our model is similar to that of Lemert and Johnston⁴⁴ except that we use the equation of state for both the liquid and vapor phases. For a given pressure we found the lowest temperature that yielded three roots to the equifugacity equation with two roots being thermodynamically stable, thus indicating two fluid phases in equilibrium with the solid phase. Figure 12 illustrates the experimental SLV data from Lemert and Johnston⁴⁴ with increasing concentrations of methanol from right to left. Also shown are the corresponding first-melting SLV curves from our Peng-Robinson model using parameters of $k_{12}=0.0230$, $k_{13}=-0.0475$, and $k_{23}=0.1675$. The model can be seen to be in good agreement with the experimental measurements, and it matches closely the model results of Lemert and Johnston⁴⁴. Note that the SLV lines with cosolvent slope upward (positive slope) so that at temperatures greater than and pressures less than the first melting SLV lines, one could observe a stable liquid phase.

We also performed the calculations for higher methanol concentrations, such as the 7.0 mole % methanol first-melting SLV curve shown in Figure 12. Based on these calculations, using a 7 mole % methanol/CO₂ solution at 35°C to extract β-naphthol should result in liquid phase formation at any pressure less than about 250 bar. The type of phase behavior, i.e., SLVE or VLE, would depend on the loading of solute. Yet, measurements identified as solid-fluid equilibrium by Dobbs and Johnston,⁴³ were as low as 120 bar for the 7.0 mole % methanol case. Once again, there are two possibilities. One possibility is that the model we have used gives a good representation of the SLV curves at 0, 2 and 4 mole % methanol but is not able to predict the 7 mole % methanol curve correctly; i.e., the model is wrong. The second possibility is that the data of Dobbs and Johnston⁴³ for 7.0 mole % methanol at 120 and 200 bar are not stable

solid-fluid equilibria. Rather, they may represent VLE data, which is not particularly meaningful without knowing the solute loading, as was discussed above in Example 1. Whichever is the case, one would certainly want to re-examine the phase behavior of the β -naphthol/CO₂/7 mole % methanol system at the lower pressures with a view cell to confirm which phases are actually present before designing an actual separation process for this system.

5.4 Computational Performance

As might be expected, the guarantee of complete reliability in computing the equilibrium state comes at some computational expense. However, for these three-component problems, the cost is actually quite small. The computation times required vary somewhat from problem to problem due to differences in the number of equilibrium phases and the number of stationary points in the phase stability analysis. The case of the CO₂-naproxen-acetone system at 333.1 K is typical. Here for the pressures yielding SLV equilibrium, the CPU times are around 30 seconds, and for pressures yielding SFE around 10 seconds (all CPU times based on using a Dell WorkStation 530MT at 2 GHz). These times are certainly much higher than what would be required by standard local methods for computing phase equilibrium. However, such standard methods offer no guarantee that the equilibrium state has actually been found. Thus, there is a trade-off between computation time and reliability, and the modeler must decide how important it is to know for certain that the correct answer has been obtained.

In the approach used here, essentially all the CPU time is spent in the phase stability analysis stage of the problem, for which, as discussed above, the interval methodology of Hua *et al.*³⁵ is used. Another approach for reliable determination of phase stability from cubic EOS models is that of Harding and Floudas⁴⁵, who use a global optimization method based on branch-and-bound using convex underestimating functions. However, this approach will not find all of

the stationary points of the tangent plane distance (useful to initialize the phase split computations) and so is not directly comparable to the approach of Hua *et al.*³⁵

6. CONCLUSIONS

We have presented a completely reliable solution strategy for computing high-pressure, solid-multiphase equilibria, using cubic equations of state. The key to this technique is the use of interval analysis to implement the thermodynamic stability test. This is an extension of our previous work on the reliable computation of solid-fluid equilibria⁷ to include the presence of cosolvents. Gaseous or liquid cosolvents are frequently used in supercritical fluid extraction processes, and are integral in processes such as the gas anti-solvent process (GAS) to precipitate uniform solid particles. Identifying the correct stable high-pressure phase equilibrium predicted by a particular model can be very problematic for commonly used local solvers. This situation is only further exacerbated when cosolvents are present. The presence of even chemical similar cosolvents can induce complex phase behavior that may not be intuitive to either the experimentalist or the modeler. Using several examples from the literature, we have demonstrated how our new solution technique, based on interval analysis, can be used to identify experimental data that may have been misinterpreted and to identify models that do not predict what the modeler intended.

7. Acknowledgements

Financial support from the Department of Energy, under Grant DE-FG02-98ER14924, the Petroleum Research Fund, administered by the ACS, under Grant 35979-AC9, the State of Indiana 21st Century Research and Technology Fund, a Bayer Predoctoral Fellowship (A.M.S.), and the University of Notre Dame Provost Fellowship (G.X.) is gratefully acknowledged.

References

- (1) McHugh, M. A.; Krukonis, V. J. *Supercritical Fluid Extraction: Principles and Practice*; 2nd ed.; Butterworth-Heinemann: Oxford, U.K., 1994.
- (2) Matson, D. W.; Fulton, J. L.; Petersen, R. X.; Smith, R. D. Rapid Expansion of Supercritical Fluid Solutions: Solute Formation of Powders, Thin Films and Fibers. *Ind. Eng. Chem. Res.* **1987**, 26, 2298-2306.
- (3) Mohamed, R. S.; Debenedetti, R. G.; Prud'homme, R. K. Effects of Process Conditions on Crystals Obtained from Supercritical Mixtures. *AIChE J.* **1987**, 35, 325-328.
- (4) Dixon, D.; Johnston, K. P. Molecular Thermodynamics of Solubilities in Gas-Antisolvent Crystallization. *AIChE J.* **1991**, 37, 1441-1449.
- (5) Gallagher, P. M.; Coffey, M. P., Krukonis, V. J.; Klasutis, N. New Process to Recrystallize Compounds Insoluble in Supercritical Fluids, in K.P. Johnston, J.M.L. Penninger (Eds.), *Supercritical Fluid Science and Technology*, American Chemical Society, Washington, DC, **1989**, p.334.
- (6) Reverchon, E. Supercritical Antisolvent Precipitation of Micro- and Nano-Particles. *J. Supercrit. Fluids* **1999**, 15, 1-21.
- (7) Xu, G.; Scurto, A. M.; Castier, M.; Brennecke, J. F.; Stadtherr, M. A. Reliable Computation of High Pressure Solid-Fluid Equilibrium. *Ind. Eng. Chem. Res.* **2000**, 39,1624-1636.
- (8) McHugh, M. A.; Paulaitis, M. E. Solid Solubilities of Naphthalene and Biphenyl in Supercritical Carbon Dioxide. *J. Chem. Eng. Data* **1980**, 29, 326-328.
- (9) McHugh, M. A.; Yogan, T. J. Three-Phase Solid-Liquid-Gas Equilibria for Three Carbon Dioxide-Hydrocarbon Solid Systems, Two Ethane-Hydrocarbon Systems, and Two Ethylene-

Hydrocarbon Solid Systems. *J. Chem. Eng. Data* **1984**, 29, 112-115.

(10) Brunner, G.; Peter, S. On the Solubility of Glycerides and Fatty Acids in Compressed Gases in the Presence of an Entrainer. *Sep. Sci. Tech.* **1982**, 17, 199-214.

(11) Joshi, D. K.; Prausnitz, J. M. Supercritical Fluid Extraction with Mixed Solvents. *AIChE J.* **1984**, 30, 522-525.

(12) Ekart, M. P.; Bennett, K. L.; Ekart, S. M.; Gurdial, G. S.; Liotta, C. L.; Eckert, C. A. Cosolvent Interactions in Supercritical Fluid Solutions. *AIChE J.* **1993**, 39, 235-248.

(13) Dobbs, J. M.; Johnston, K. P. Selectivities in Pure and Mixed Supercritical Fluid Solvents. *Ind. Eng. Chem. Res.* **1987**, 26, 1476-1482.

(14) Jessop, P. G.; Ikariya, T.; Noyori, R. Homogeneous Catalysis in Supercritical Fluids. *Chem. Rev.* **1999**, 99, 475-493.

(15) De Swaans Arons, J.; Diepen, G. A. M. Thermodynamic Study of Melting Equilibria under Pressure of a Supercritical Gas. *Rec. Trav. Chim. Pays-Bas* **1963**, 82, 249-256.

(16) Luks, K. D. The Occurrence and Measurement of Multiphase Equilibria Behavior. *Fluid Phase Equil.* **1986**, 29, 209-224.

(17) van Welie, G. S. A.; Diepen, G. A. M. The solubility of Naphthalene in Supercritical Ethane. *J. Phys. Chem.* **1963**, 67, 755-757.

(18) Smith, G. R.; Wormald, C. J. Solubilities of Naphthalene in (CO₂ + C₂H₆) and (CO₂ + C₃H₈) up to 333 K and 17.7 MPa. *Fluid Phase Equil.* **1990**, 57, 205-222.

(19) Koningsveld, R., Diepen, G. A. M. Supercritical Phase Equilibrium Involving Solids. *Fluid Phase Equil.* **1983**, 10, 159-172.

- (20) Kikic, I.; Lora, M.; Bertucco, A. A. Thermodynamic Analysis of Three-Phase Equilibria in Binary and Ternary Systems for Applications in Rapid Expansion of a Supercritical Solution (RESS), Particles from Gas-Saturated Solutions (PGSS), and Supercritical Antisolvent (SAS). *Ind. Eng. Chem. Res.* **1999**, *36*, 5507-5515.
- (21) Lemert, R. M.; Johnston, K. P. Solid-Liquid-Gas Equilibria in Multicomponent Supercritical Fluid Systems. *Fluid Phase Equil.* **1989**, *45*, 265-286.
- (22) Da Rocha, S. R. P.; Oliveira, J. V.; d'Ávila, S. G. A. Three-Phase Ternary Model for CO₂-Solid-Liquid Equilibrium at Moderate Pressures. *J. Supercrit. Fluids* **1996**, *8*, 1-5.
- (23) Baker, L. E.; Pierce, A. C.; Luks, K. D. Gibbs Energy Analysis of Phase Equilibria. *Soc. Pet. Eng. J.* **1982**, *22*, 731-742.
- (24) Marcilla, A.; Conesa, J. A.; Olaya, M. M. Comments on the Problematic Nature of the Calculation of Solid-Liquid Equilibrium. *Fluid Phase Equil.* **1997**, *135*, 169-175.
- (25) Lucia, A.; Padmanabhan, L.; Venkataraman, S. Multiphase Equilibrium Flash Calculations. *Comput. Chem. Eng.* **2000**, *24*, 2557-2569.
- (26) Zhou, X.; Thomas, F. B.; Moore, R. G. Modeling of Solid Precipitation from Reservoir Fluid. *J. Can. Pet. Tech.* **1996**, *35*, 37-45.
- (27) Chen, H. S.; Stadtherr, M. A. Enhancements of the Han-Powell Method for Successive Quadratic Programming. *Comput. Chem. Eng.* **1984**, *8*, 229-234.
- (28) Michelsen, M. L. The Isothermal Flash Problem. 1. Stability. *Fluid Phase Equil.* **1982**, *9*, 1-19.
- (29) Michelsen, M. L. The Isothermal Flash Problem. 2. Phase-Split Calculation. *Fluid Phase*

Equil. **1982**, 9, 21-40.

(30) McKinnon, K. I. M.; Millar, C. G.; Mongeau M. Global Optimization for the Chemical and Phase Equilibrium Problem Using Interval Analysis. In *State of the Art in Global Optimization: Computational Methods and Applications*; Floudas, C. A.; Pardalos, P.M., Eds.; Kluwer Academic Publishers: Dordrecht, The Netherlands, 1996.

(31) Neumaier, A. *Interval Methods for Systems of Equations*; Cambridge University Press: Cambridge, England, 1990.

(32) Hansen, E. *Global Optimization Using Interval Analysis*, Marcel Dekkar: New York, 1992.

(33) Kearfott, R. B. 1996, *Rigorous Global Search: Continuous Problems*; Kluwer Academic Publishers: Dordrecht, The Netherlands.

(34) Hua, J. Z.; Brennecke, J. F.; Stadtherr, M. A. Reliable Computation of Phase Stability Using Interval Analysis: Cubic Equation of State Models. *Comput. Chem. Eng.* **1998**, 22, 1207-1214.

(35) Hua, J. Z.; Brennecke, J. F.; Stadtherr, M. A. Enhanced Interval Analysis for Phase Stability: Cubic Equation of State Models. *Ind Eng. Chem. Res.* **1998**, 37, 1519-1527.

(36) Schnepper, C. A.; Stadtherr, M. A. Robust Process Simulation Using Interval Methods. *Comput. Chem. Eng.*, **1996** 20, 187-199.

(37) Stradi, B. A.; Brennecke, J. F.; Kohn, J. P.; Stadtherr, M. A. Reliable Computation of Mixture Critical Points. *AIChE J.* **2001**, 47, 212-221.

(38) Maier, R. W.; Brennecke, J. F.; Stadtherr, M. A. Computing Homogeneous Azeotropes Using Interval Analysis. *Chem. Eng. Technol.* **1999**, 22, 1063-1067.

- (39) Hua, J. Z. Interval Methods for Reliable Computation of Phase Equilibrium from Equation of State Models, Ph.D. Thesis, University of Illinois, Urbana, Illinois, 1997.
- (40) Stradi, B. A.; Xu, G.; Brennecke, J. F.; Stadtherr, M. A. Modeling and Design of an Environmentally Benign Reaction Process. *AIChE Symp. Ser.* **2000**, *96*, 371-375.
- (41) Ting, S. S. T.; Macnaughton, S. J.; Tomasko, D. L.; Foster, N. R. Solubility of Naproxen in Supercritical Carbon Dioxide with and without Cosolvents. *Ind. Eng. Chem. Res.* **1993**, *32*, 1471-1481.
- (42) Dobbs, J. M.; Wong, J. M.; Lahiere, R. J.; Johnston, K. P. Modification of Supercritical Fluid Phase Behavior Using Polar Cosolvents. *Ind. Eng. Chem. Res.* **1987**, *26*, 56-65.
- (43) Dobbs, J. M.; Johnston, K. P. Selectivities in Pure and Mixed Supercritical Fluid Solvents. *Ind. Eng. Chem. Res.* **1987**, *26*, 1476-1482.
- (44) Lemert, R. M.; Johnston, K. P. Solid-Liquid-Gas Equilibria in Multicomponent Supercritical Fluid Systems. *Fluid Phase Equil.* **1989**, *45*, 265-286.
- (45) Harding, S. T.; Floudas, C. A. Phase Stability with Cubic Equations of State: Global Optimization Approach. *AIChE J.* **2000**, *46*, 1422-1440.

Table 1. Physical property values.

Compound	T_c [K]	P_c [bar]	ω	v^S [cm ³ /mol]	Δh^{fus} [kJ/mol]	T_m [K]
CO ₂	304.25	73.8	0.225			
C ₂ H ₆	305.35	48.8	0.098			
C ₃ H ₈	369.82	42.5	0.154			
Acetone	508.20	46.6	0.318			
Methanol	512.60	80.9	0.556			
Naphthalene	748.40	40.5	0.302	109.1	189.98	353.45
Naproxen ^a	807.00	24.2	0.904	178.3		
β -Naphthol	824.85	42.9	0.468	116.7	107.44	395.65

^a Sublimation pressure $P_2^{sub} = 38.8 \times 10^{-8}$ bar at 333.1 K.

Table 2. Phase equilibrium of naproxen in CO₂ with acetone cosolvent ($\alpha_3 = 96.5/3.5$) at 333.1 K and solute loading $\psi_2 = 0.25$.

Pressure [bar]	Experimental ^a $y_2 \times 10^5$	Computed Phase Equilibrium ^b						
		<u>Fluid</u> $y_2 \times 10^5$	<u>Fluid</u> v^V	<u>Fluid</u> β^V	<u>Liquid</u> x_2	<u>Liquid</u> v^L	<u>Liquid</u> β^L	<u>Solid</u> β^S
110.3	2.03	0.70	113.3	0.72321	0.411	133.4	0.04549	0.23130
124.1	3.42	2.17	88.63	0.73213	0.402	131.6	0.02991	0.23796
137.9	5.37	4.30	76.85	0.74035	0.394	130.0	0.01598	0.24367
151.7	6.96	6.57	70.46	0.74707	0.387	128.6	0.00485	0.24807
165.5	8.55	8.24	66.59	0.75006	-	-	-	0.24994
179.3	10.8	9.16	63.90	0.75007	-	-	-	0.24993

^a Fluid phase solubility [mole fraction] of naproxen in the “solid-fluid equilibrium” measured by Ting *et al.*⁴¹ with unspecified solute loading.

^b Here y_2 and x_2 are the solubilities [mole fraction] of naproxen in the fluid and liquid phases, respectively; v^V and v^L are the molar volumes [cm³/mol] of the fluid and liquid phases, respectively; β^V , β^L , β^S are the phase fractions for the fluid, liquid and solid phases, respectively.

Figure Captions

Figure 1. Pressure-temperature (PT) projection of a typical asymmetric system in supercritical fluid extraction. I and II represent two different possibilities for the upper SLV equilibrium.

Figure 2. One typical scenario for liquid phase formation in solid-fluid extraction using a cosolvent.

Figure 3. A ternary composition diagram illustrating pressure P_A (see Fig. 2). The dashed line represents overall feed compositions with a constant solvent/cosolvent loading. Diagram is not to scale.

Figure 4. A ternary composition diagram illustrating pressure P_B (see Fig. 2). The dashed line represents overall feed compositions with a constant solvent/cosolvent loading. Diagram is not to scale.

Figure 5. A ternary composition diagram illustrating pressure P_C (see Fig. 2). The dashed line represents overall feed compositions with a constant solvent/cosolvent loading. Diagram is not to scale.

Figure 6. A ternary composition diagram illustrating pressure P_D (see Fig. 2). The dashed line represents overall feed compositions with a constant solvent/cosolvent loading. Box *a* shows the case if the temperature of the system is changed to above the binary SLV line of the naphthalene/ CO_2 system. Diagram is not to scale.

Figure 7. Computed solubility of naphthalene in $\text{CO}_2/\text{C}_2\text{H}_6$ ($\alpha_3 = 0.7$) at $T = 307.9$ K, along with the data of Smith and Wormald.¹⁸

Figure 8. Computed solubility of naphthalene in CO₂/C₂H₆ ($\alpha_3 = 0.7$) at $T = 323$ K, along with the data of Smith and Wormald.¹⁸ See text for discussion.

Figure 9. Computed solubility of naphthalene in CO₂/C₂H₆ ($\alpha_3 = 0.7$) at $T = 333$ K, along with the data of Smith and Wormald.¹⁸ See text for discussion.

Figure 10. Computed solubility of naphthalene in CO₂/C₃H₈ ($\alpha_3 = 5.6$) at $T = 308.3$ K, along with the data of Smith and Wormald.¹⁸

Figure 11. Computed solubility of naphthalene in CO₂/C₃H₈ ($\alpha_3 = 5.6$) at $T = 328.3$ K, along with the data of Smith and Wormald.¹⁸ See text for discussion.

Figure 12. PT projection for β -naphthol and CO₂ with methanol cosolvent, illustrating SLV equilibrium (“first melting” lines) at various cosolvent loadings, as measured by Lemert and Johnston⁴⁴ (open squares at 4% methanol; open diamonds at 2% methanol; solid squares at 0% methanol) and as computed from the Peng-Robinson EOS (solid lines). Also shown (open circles) are points where Dobbs and Johnston⁴³ report making “solid-fluid equilibrium” measurements at 7% methanol. See text for discussion.

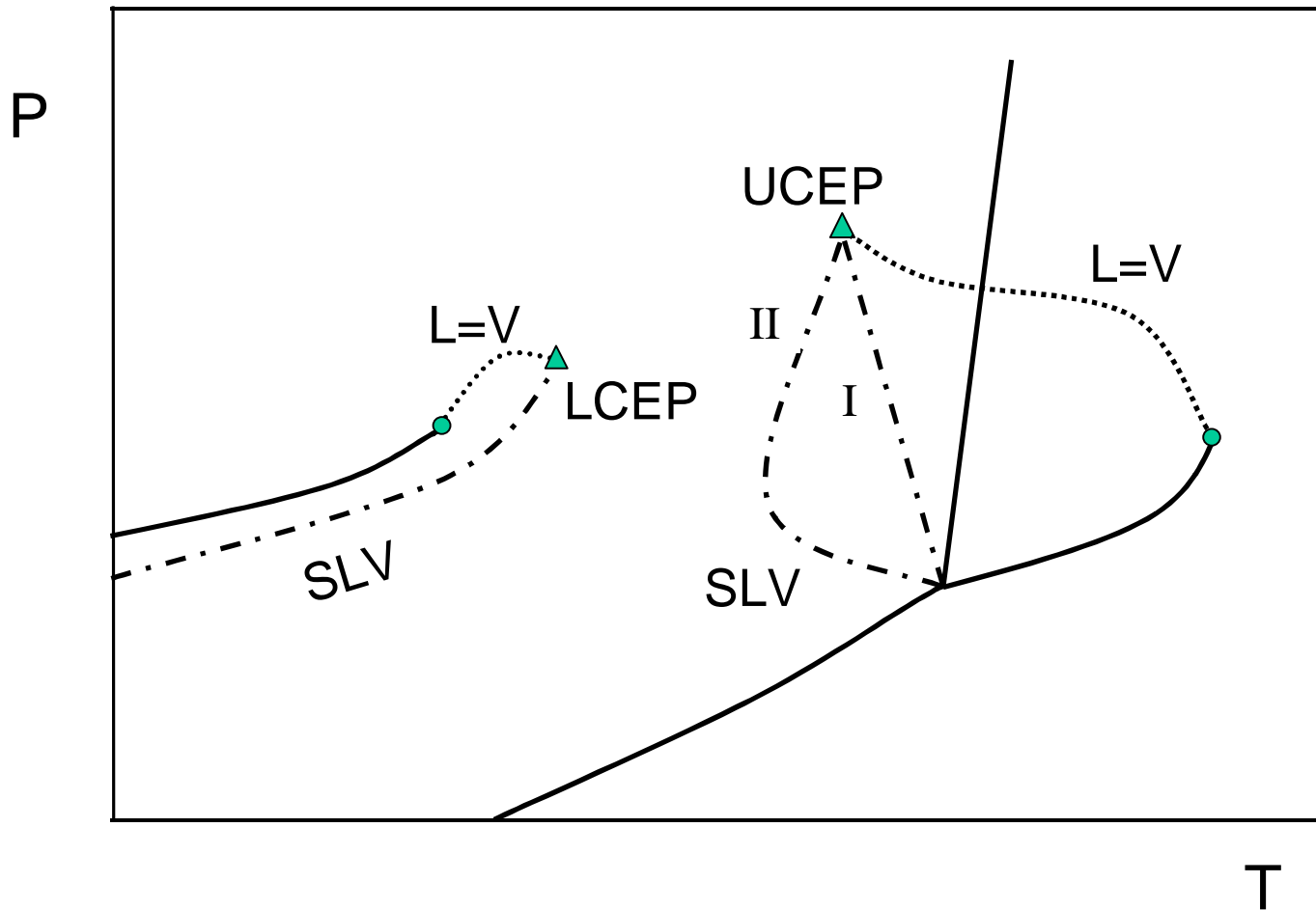


Figure 1. Pressure-temperature (PT) projection of a typical asymmetric system in supercritical fluid extraction. I and II represent two different possibilities for the upper SLV equilibrium.

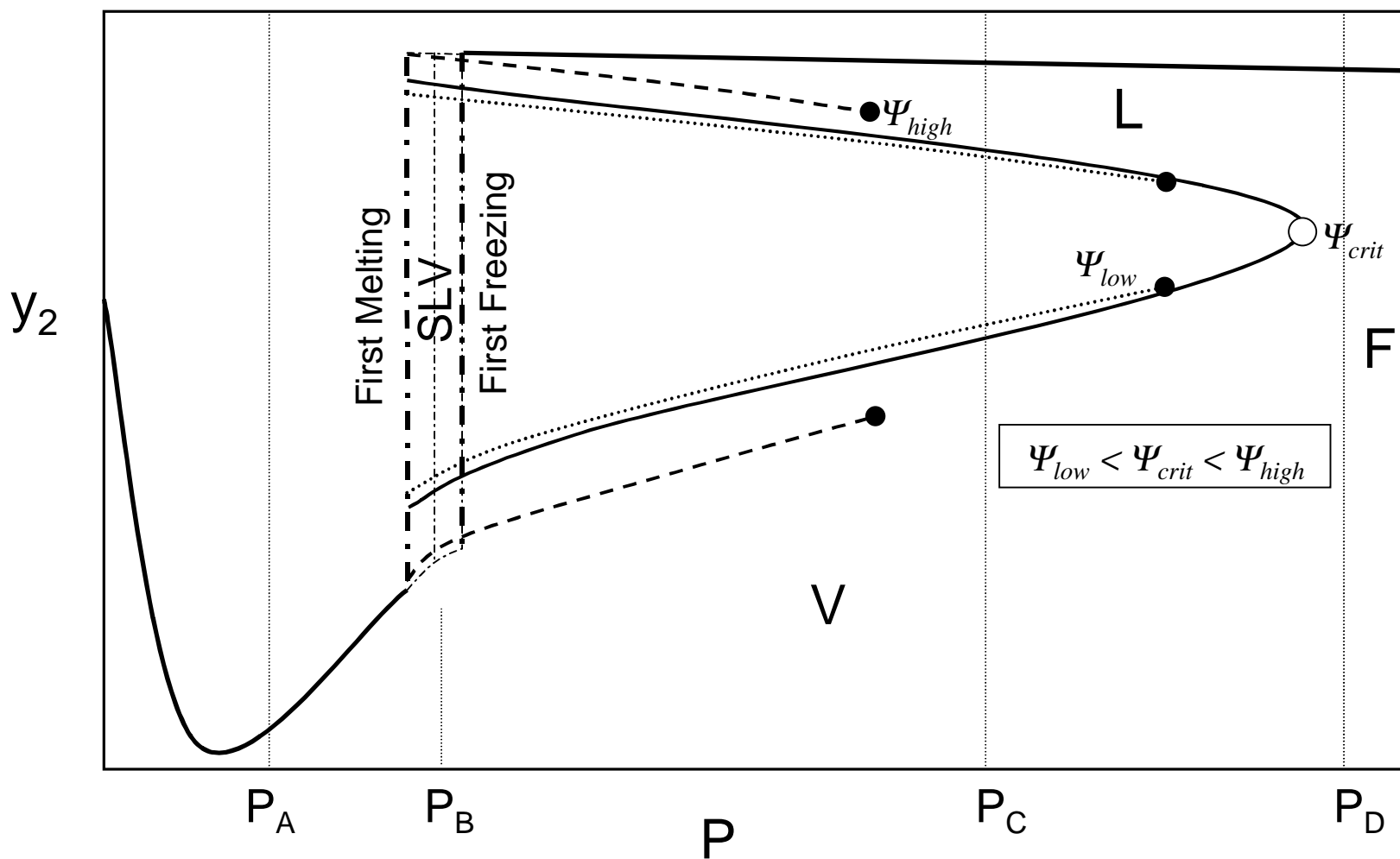


Figure 2. One typical scenario for liquid phase formation in solid-fluid extraction using a cosolvent.

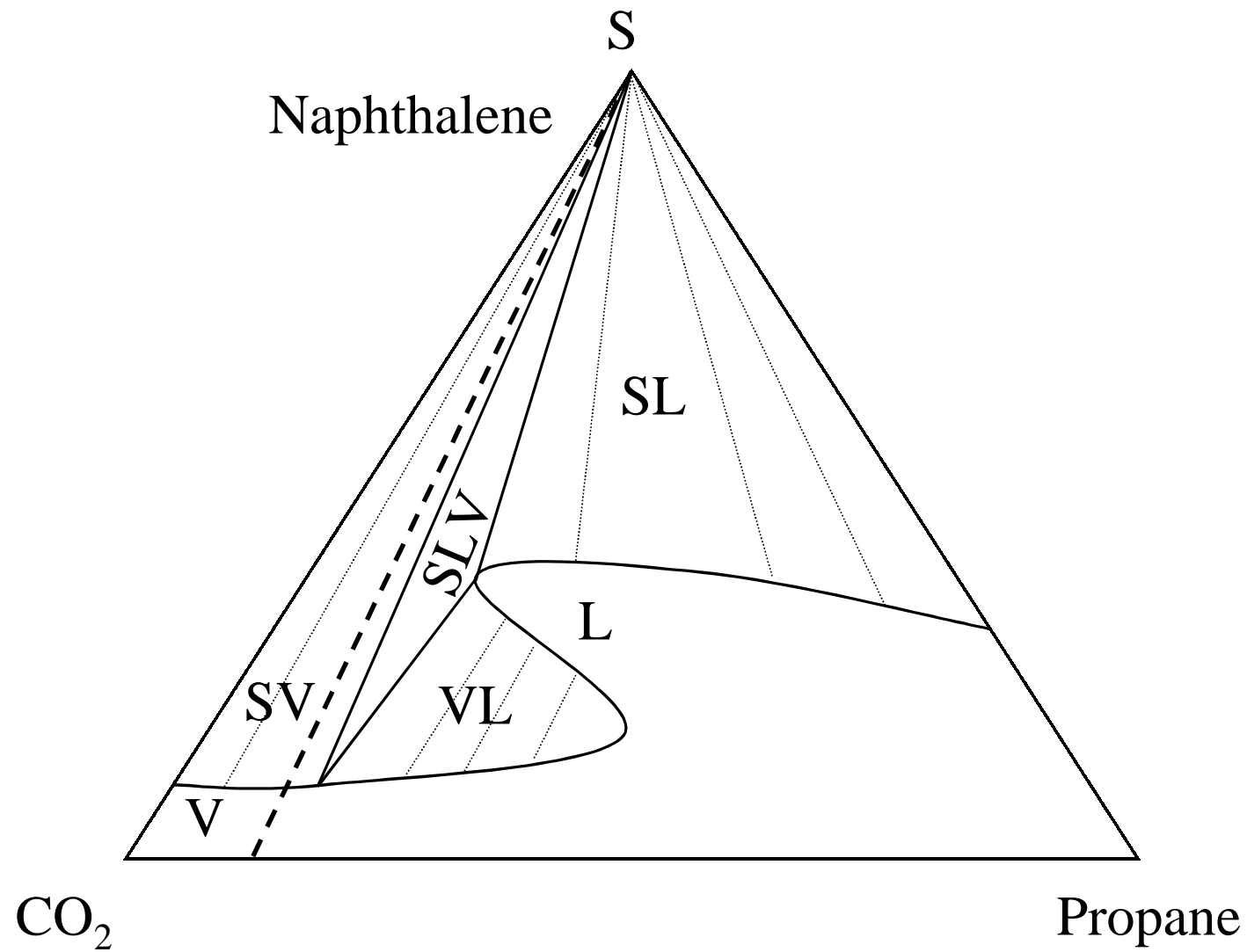


Figure 3. A ternary composition diagram illustrating pressure P_A (see Fig. 2). The dashed line represents overall feed compositions with a constant solvent/cosolvent loading. Diagram is not to scale.

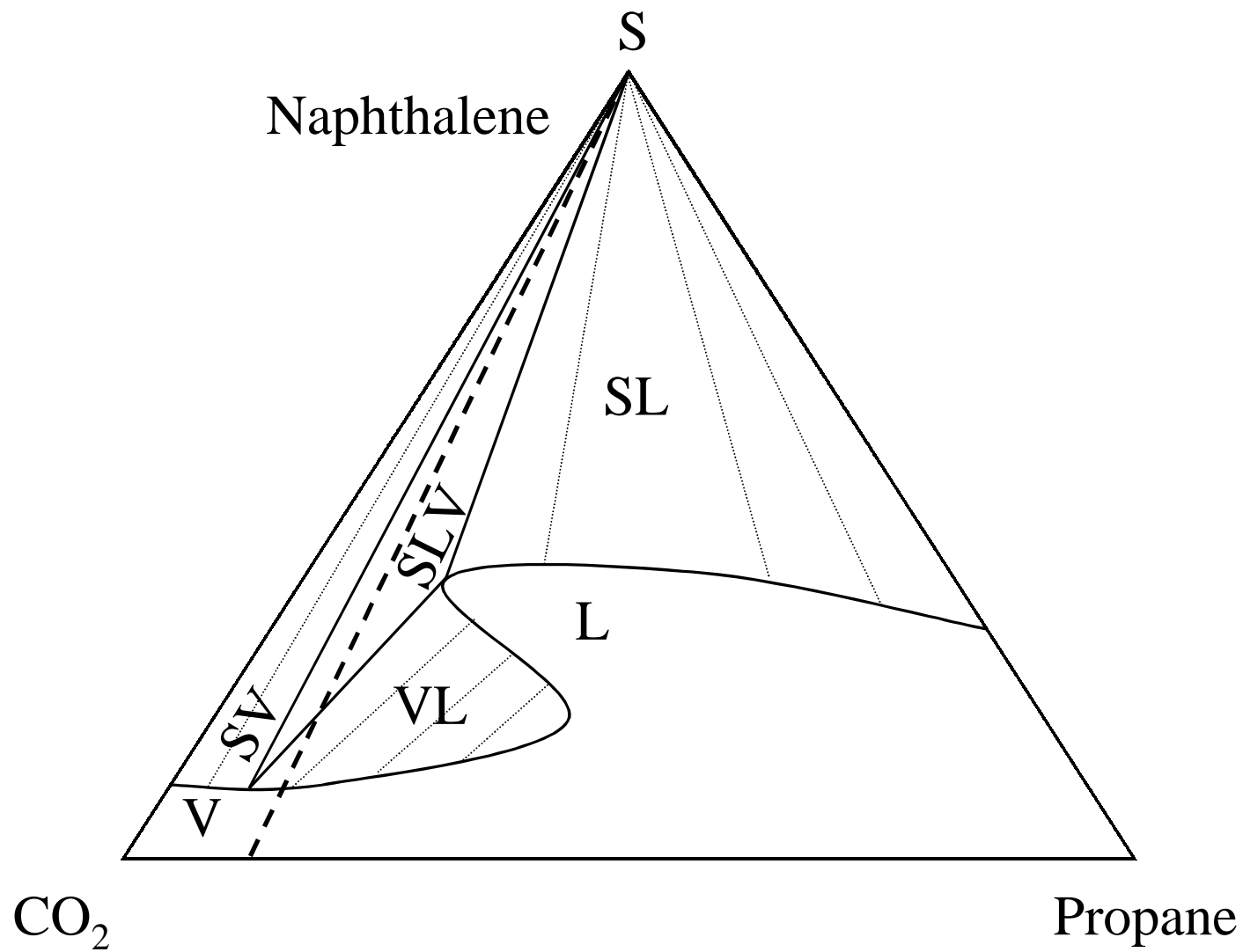


Figure 4. A ternary composition diagram illustrating pressure P_B (see Fig. 2). The dashed line represents overall feed compositions with a constant solvent/cosolvent loading. Diagram is not to scale.

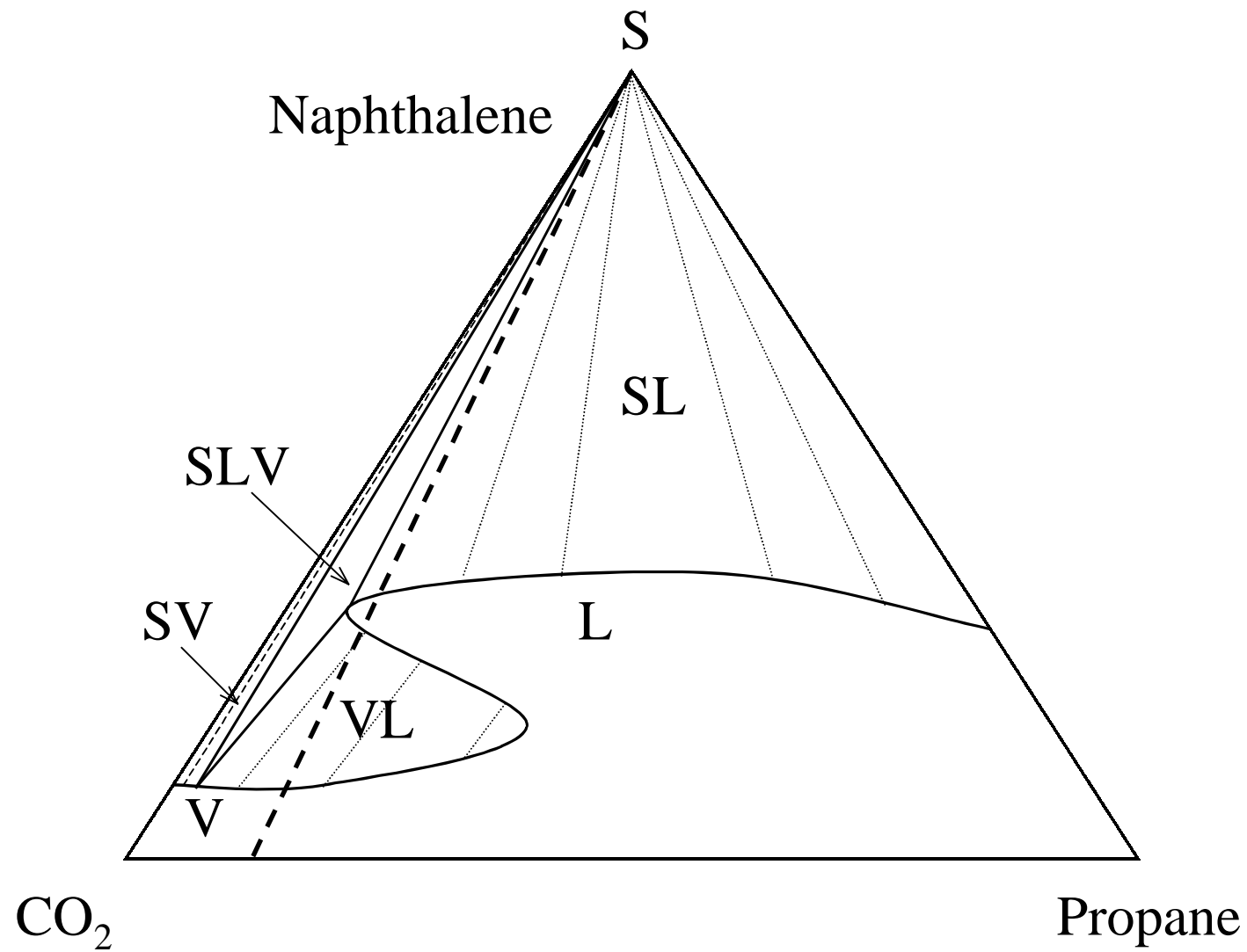


Figure 5. A ternary composition diagram illustrating pressure P_C (see Fig. 2). The dashed line represents overall feed compositions with a constant solvent/cosolvent loading. Diagram is not to scale.

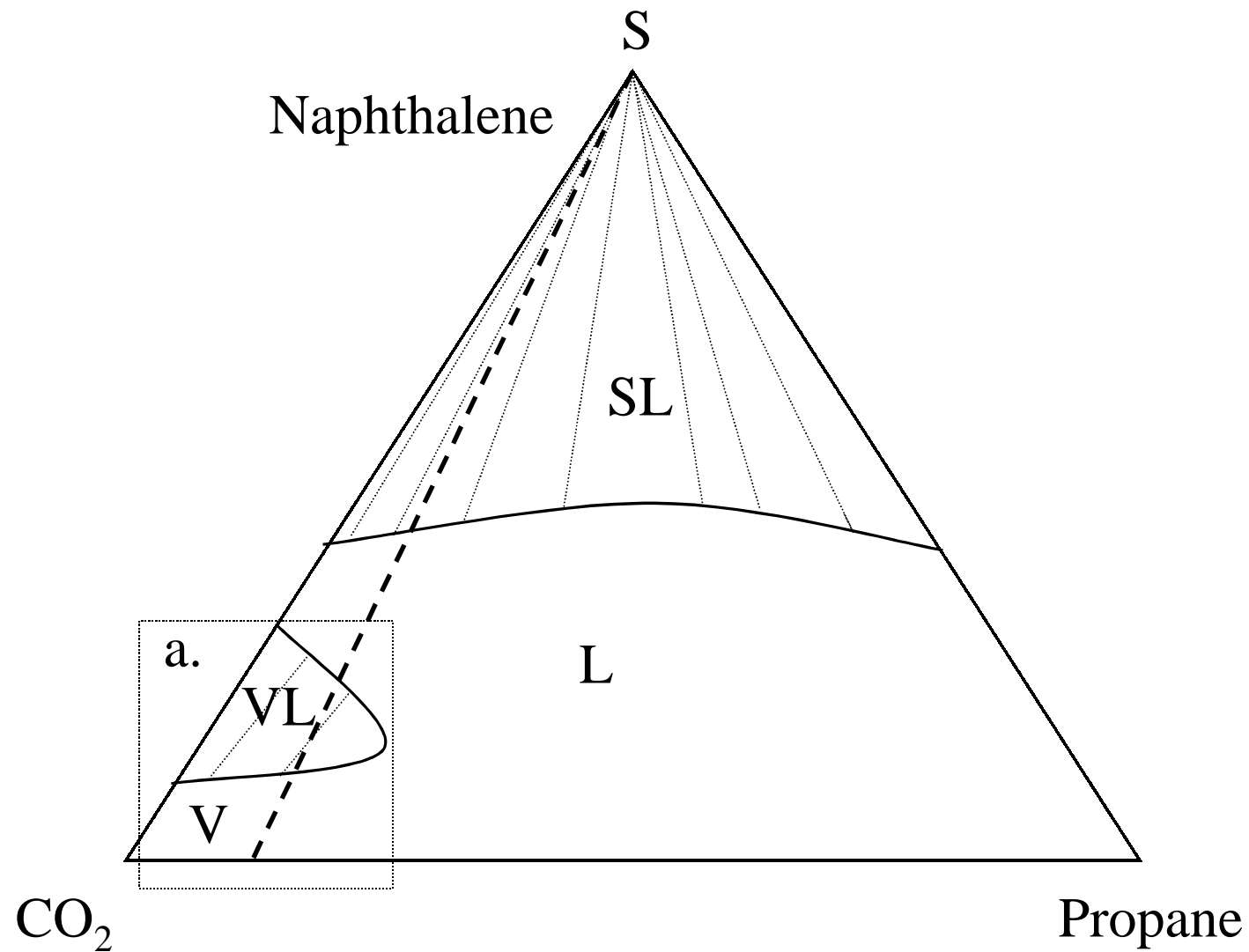


Figure 6. A ternary composition diagram illustrating pressure P_D (see Fig. 2). The dashed line represents overall feed compositions with a constant solvent/cosolvent loading. Box *a* shows the case if the temperature of the system is changed to above the binary SLV line of the naphthalene/CO₂ system. Diagram is not to scale.

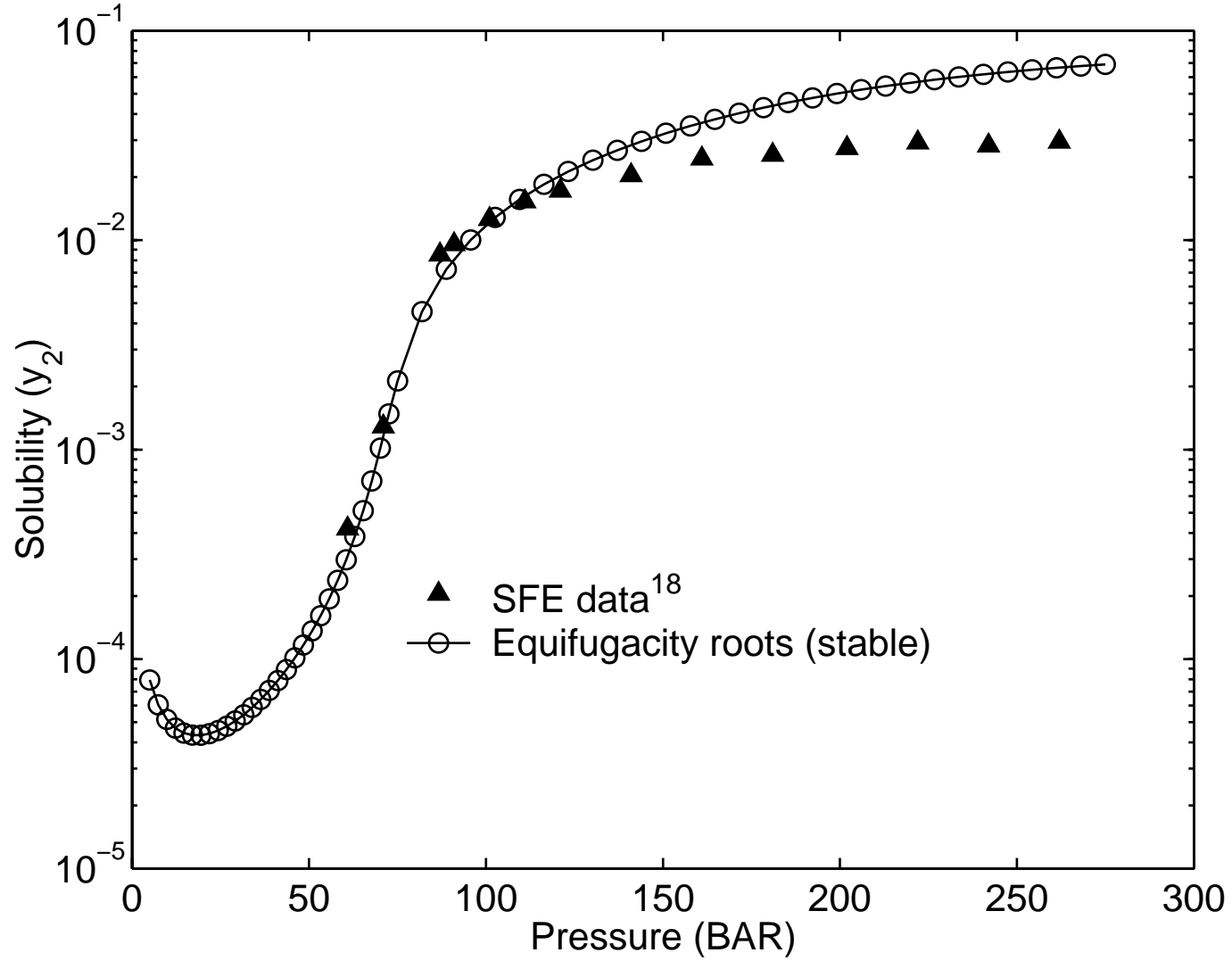


Figure 7. Computed solubility of naphthalene in $\text{CO}_2/\text{C}_2\text{H}_6$ ($\alpha_3 = 0.7$) at $T = 307.9$ K, along with the data of Smith and Wormald.¹⁸

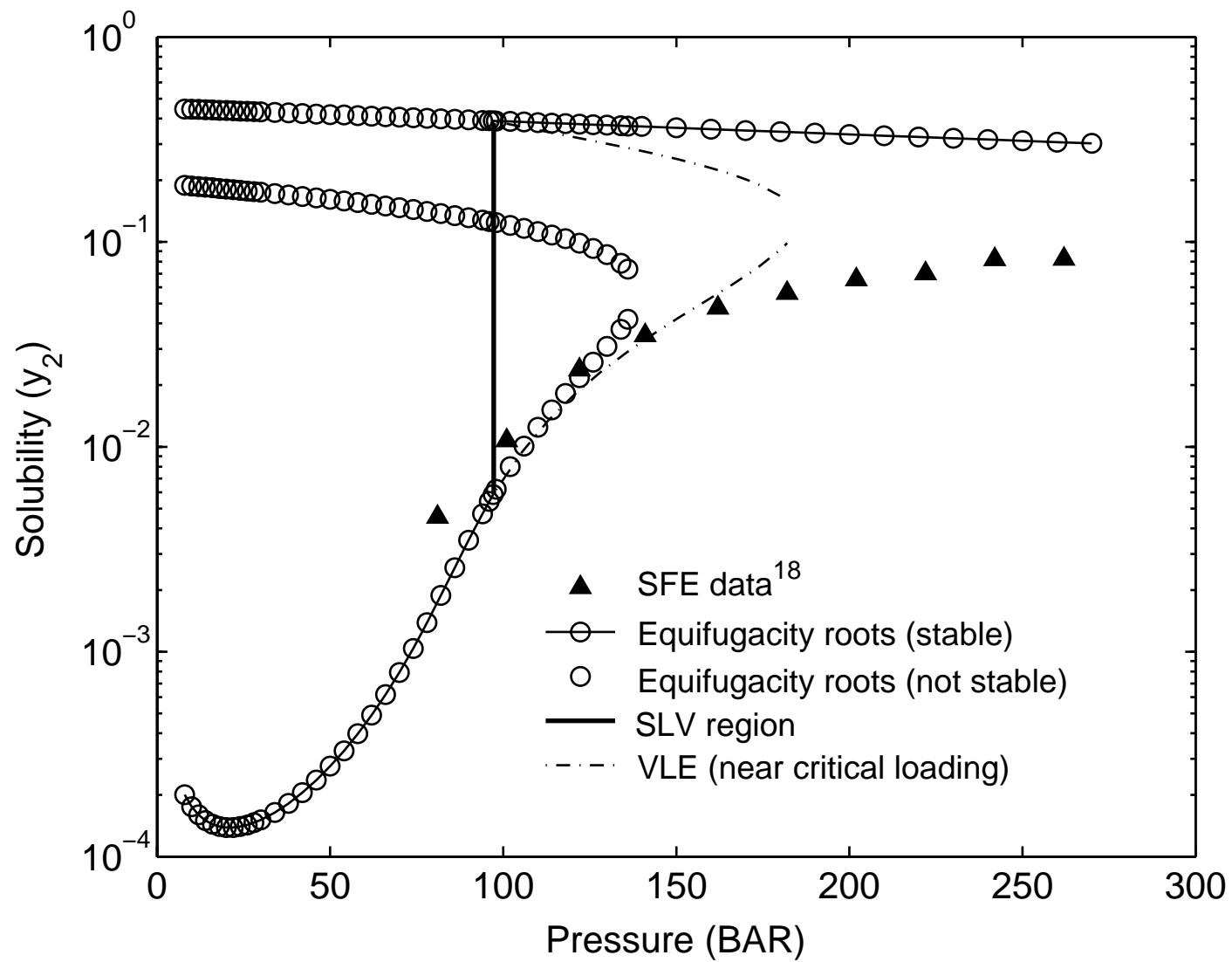


Figure 8. Computed solubility of naphthalene in CO₂/C₂H₆ ($\alpha_3 = 0.7$) at $T = 323$ K, along with the data of Smith and Wormald.¹⁸ See text for discussion.

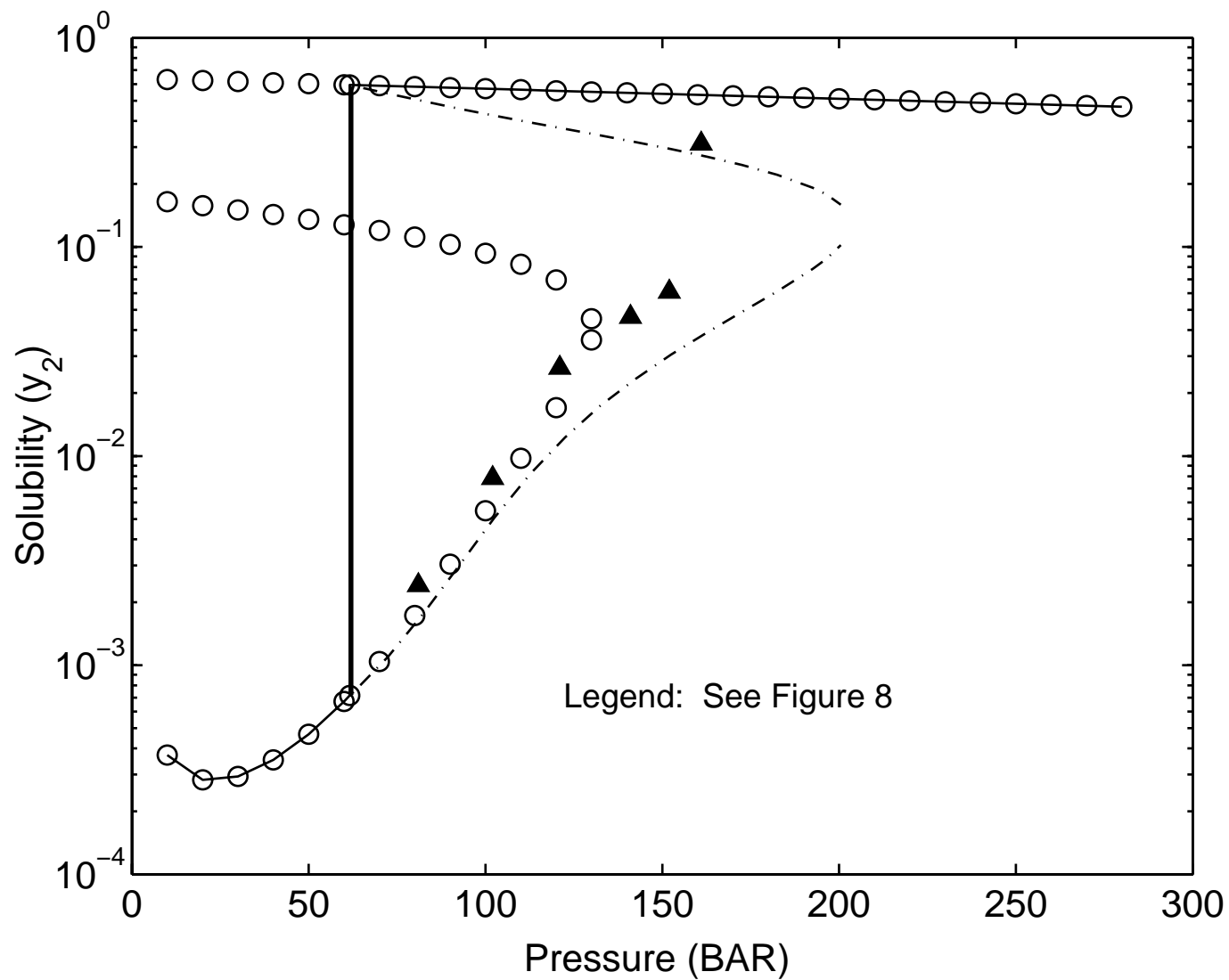


Figure 9. Computed solubility of naphthalene in $\text{CO}_2/\text{C}_2\text{H}_6$ ($\alpha_3 = 0.7$) at $T = 333$ K, along with the data of Smith and Wormald.¹⁸ See text for discussion.

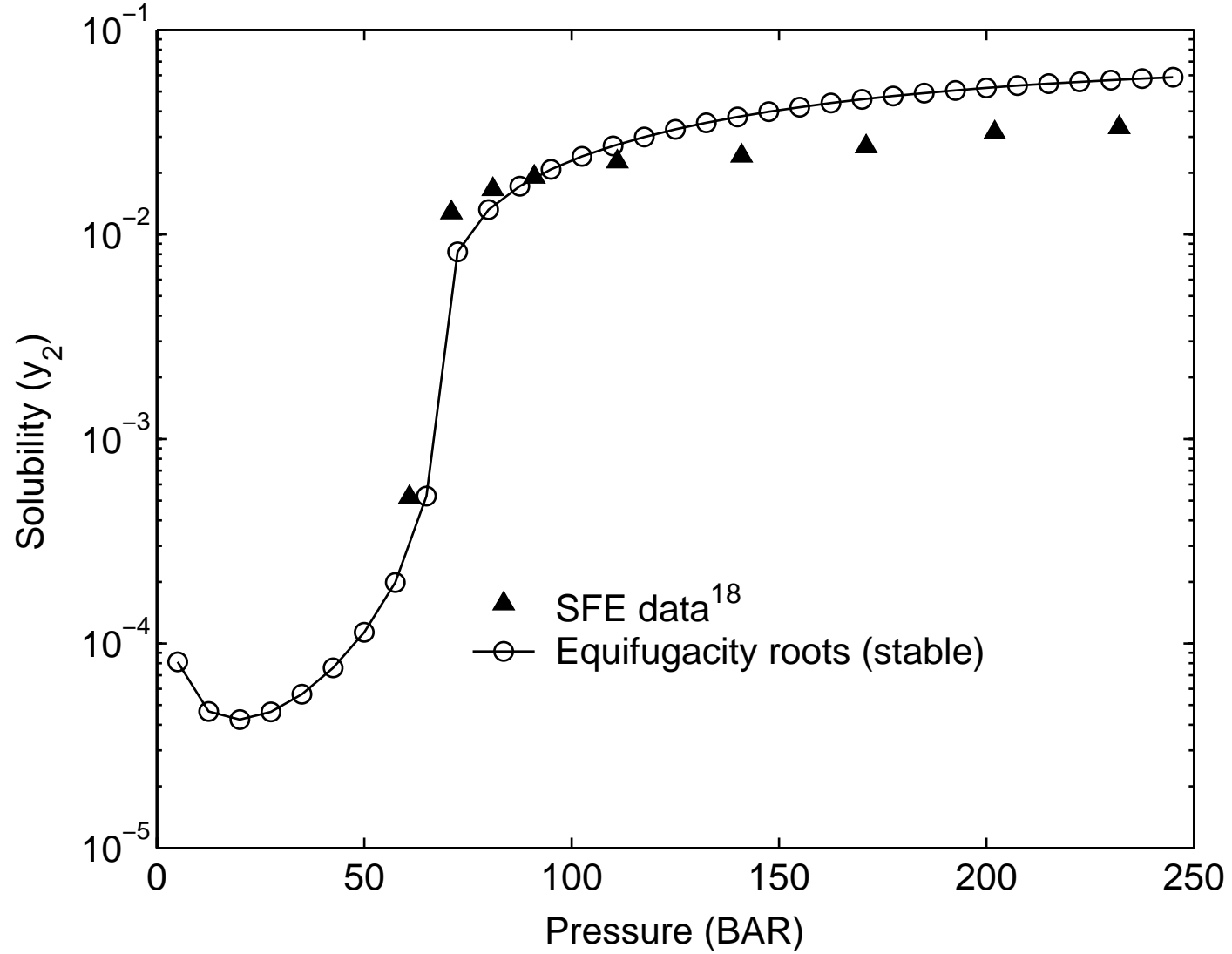


Figure 10. Computed solubility of naphthalene in $\text{CO}_2/\text{C}_3\text{H}_8$ ($\alpha_3 = 5.6$) at $T = 308.3$ K, along with the data of Smith and Wormald.¹⁸

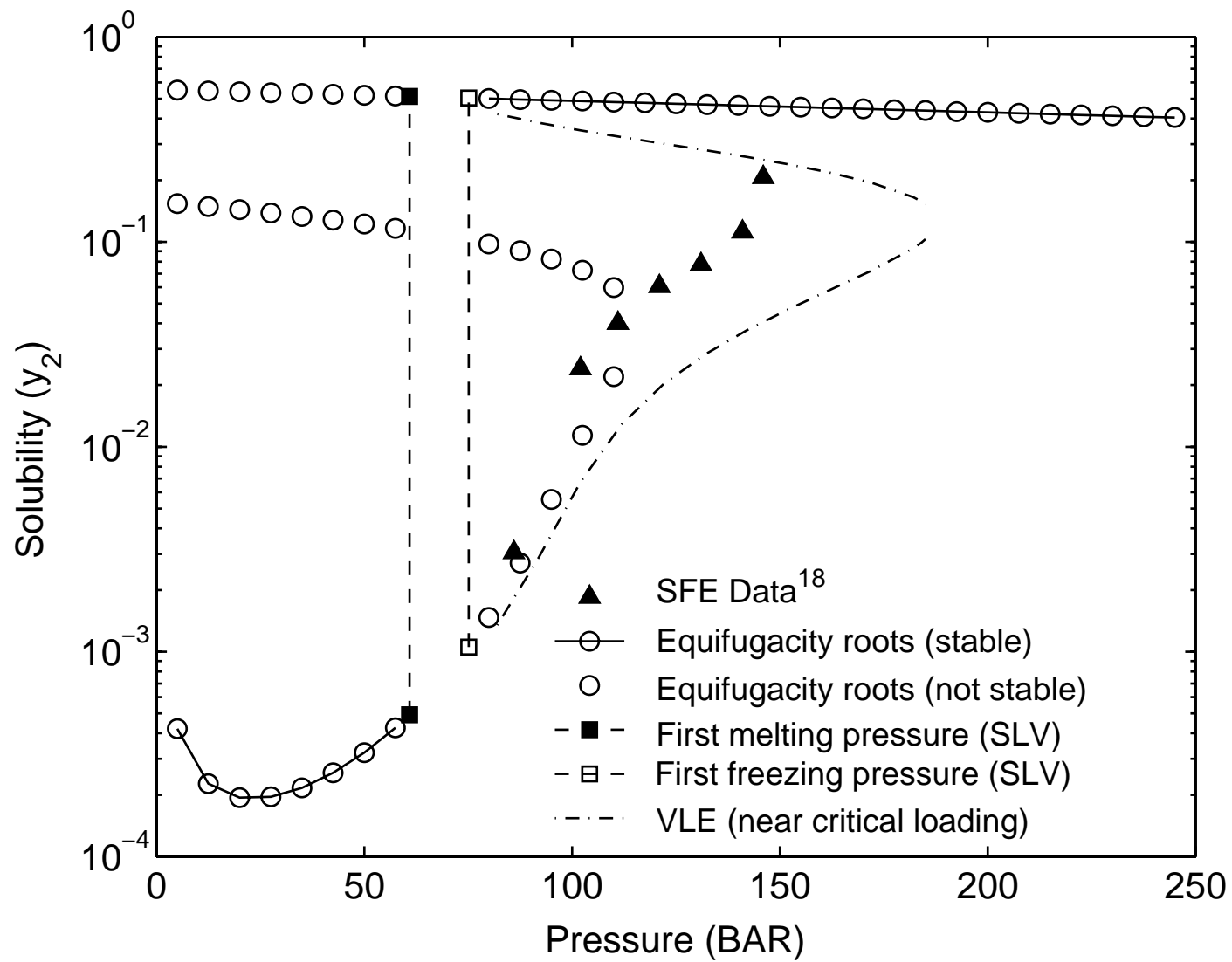


Figure 11. Computed solubility of naphthalene in CO₂/C₃H₈ ($\alpha_3 = 5.6$) at $T = 328.3$ K, along with the data of Smith and Wormald.¹⁸ See text for discussion.

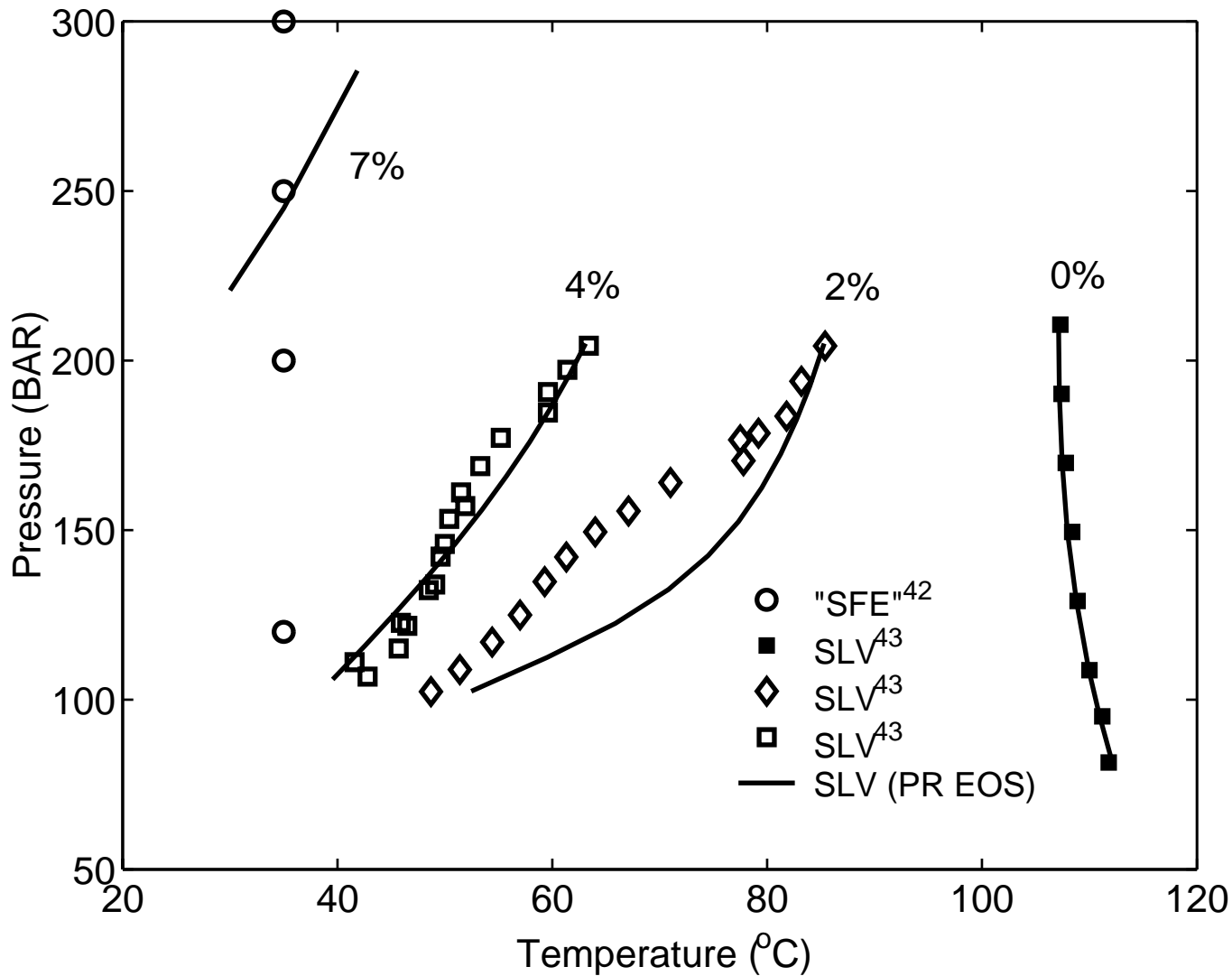


Figure 12. PT projection for β -naphthol and CO_2 with methanol cosolvent, illustrating SLV equilibrium (“first melting” lines) at various cosolvent loadings, as measured by Lemert and Johnston⁴⁴ (open squares at 4% methanol; open diamonds at 2% methanol; solid squares at 0% methanol) and as computed from the Peng-Robinson EOS (solid lines). Also shown (open circles) are points where Dobbs and Johnston⁴³ report making “solid-fluid equilibrium” measurements at 7% methanol. See text for discussion.